5-2016

Evaluation of Next Generation Capillary-Channeled Polymer Fibers and the Implementation of C-CP Fiber Modification Modalities on Non-Fiber Substrates

Paul Haupt-Renaud
Clemson University, phauptr@clemson.edu

EVALUATION OF NEXT GENERATION CAPILLARY-CHANNELED POLYMER FIBERS AND THE IMPLEMENTATION OF C-CP FIBER MODIFICATION MODALITIES ON NON-FIBER SUBSTRATES

A Thesis
Presented to
the Graduate School of
Clemson University

In Partial Fulfillment
of the Requirements for the Degree
Master of Science
Chemistry

---

by
Paul Haupt-Renaud
May 2016

Accepted by:
Dr. R. Kenneth Marcus, Committee
Chair Dr. Jeffry Anker
Dr. Carlos Garcia

ABSTRACT

Developing new stationary phases for liquid chromatography is continuing to drive high performance liquid chromatography (HPLC) into the future. In this regard the Marcus' group has been leveraging the continued advances of Capillary-Channeled Polymer (C-CP) fibers in an attempt to meet the demand of high throughput biomarcomolecule chromatography. Separation mechanisms studied include: ion-exchange (IC), reversed phase (RP), affinity, hydrophobic interaction chromatography (HIC).

In this work, the next generation of C-CP fiber stationary phases was thoroughly evaluated with respect to hydrodynamic concerns relating to protein chromatography. Traditionally C-CP fibers have eight channels that run co-linearly along the length of the fiber. Packed C-CP fibers form a network of pseudo-open capillary structures through channels interdigitating. The fibers studied have a much higher surface area to volume ratio compared to circular fibers with similar diameters. The open tubular network has an added bonus of operating at low back pressures. C-CP fibers are non-porous with regards to biomarcomolecules, resulting in fast mass transfer kinetics causing no significant C-term band broadening. The next generation of C-CP fiber has been developed with three larger more ridged channels. This design allows for tighter packing densities without compromising channel integrity. This advancement allows the fibers to operate at higher linear velocities leading to a separation of a six-protein

suit (ribonuclease A, cytochrome C, lysozyme, transferrin, bovine serum albumin, and α-chimotrypsinogen) under reversed phase conditions.

Surface modification of the C-CP fibers has been accomplished with a variety of techniques, both through covalent and physical adsorption modification. Of particular interest to this work is the Lipid Tethered Ligand (LTL) surface modification modality, which has seen excellent success when employed on polypropylene C-CP fibers. LTLs functionalize a surface with ion-exchange or affinity ligands through hydrophobic physical adsorption to augment the available surface chemistry in a quick and simple flow-through system. In the work presented here, the LTL system was applied to the most commonly used polymer resin, polystyrene-divinylbenzene. The effectiveness of LTL loading, stability, and kinetics on PS-DVB was evaluated. Ligand availability was evaluated with both biotin-LTL for the extraction of streptavidin and iminodiacetic acid-LTL for the extraction of methylene blue.

TABLE OF CONTENTS

LIST OF TABLES

Table Page

LIST OF FIGURES

CHAPTER ONE

Introduction

Chromatography encompasses a broad group of techniques and methods that operate on a single simple principle, the transport of sample in a mobile phase through a stationary phase. Separation of different analytes in a given sample is achieved through differences in chemical or physical interactions at the mobile phase/solid phase interface. One of the largest areas of growth in the separation science arena is in protein and biomarcomolecule chromatography[1]. The drive in this field originates in the need for faster, better, more effective way to purify proteins for the use in biotherapeutics[2,3], and biochemical research. Every classification of biomolecule has led to its own field of study including proteomics, genomic, lipidomics, etc. Each generates its own unique analytical challenge for identification, purification and quantification. The discovery of the importance of proteins in both the study of biodiversity and biological function has created a whole field of proteomics dedicated to elucidating what roles proteins serve in biological function[4]. Proper chromatographic methods allow us the ability to study what proteins are present, and the ability to draw conclusions by monitoring them over time. The applications of protein monitoring in medicine and diagnostics are unfathomable, giving the medical community new diagnostics based on abnormal levels/ complete absence or presence of a protein to diagnose disease[5,6]. As these fields grow, the demand to purify and

identify individual molecules for study is ever increasing the demands on traditional chromatographic methods.

The development and application of polymer stationary phases is critical for the future of biomarcomolecule separations. One of the most powerful parameters that a chromatographer can change is the pH of the solvent system. This can be done stepwise as commonly seen in affinity based purification methods including Immobilized Metal Affinity Chromatography (IMAC)[7], enzymatic inhibitor affinity[8], and lectin based separation of specific hormones[9] and glycosylated proteins[10,11]. The pH can be used in a gradient for Ion Exchange Chromatography (IC)[12]. Even Reversed Phase (RP)[13], Hydrophilic Interaction Liquid Chromatography (HILIC)[14], and Size Exclusion Chromatography (SEC)[15] all rely on the modulation of the pH to tune electrostatic interactions. Although micro-particulate silica based phases have had enormous amounts of success[16], the pH stability of silica phases for bioprocessing is a constant hurtle[17]. Organic polymers have far superior pH stability when compared to silica[12], and as a result are preferable for the extreme pH conditions used in bioprocessing.

The most widely used polymers stationary phases are poly(vinylalcohol)[18], poly(methylacryate)[19], poly(ethylvinylbenzene-divinylbenzene)[20], and poly(styrene)-divinylbenzene[21]. Of these, the poly-aromatic stationary phases are considered preferable because they remain chemically stable in the entire aqueous pH range. Polymer stationary phases are currently employed because

the stationary phase will not begin to irreversibly bind bio-active molecule as the column ages[22]. The stability of micro-particulate silica exposed to carbonate or phosphate buffers, commonly used in bioprocessing, has been seen sensitize the silica to basic conditions[23]. Poly-aromatics have the added benefit of simple functionalization both covalently to the benzene ring[24], and non-covalently through adsorption of appropriate small molecules[25].

The Marcus' group has been developing Capillary-Channeled Polymer (C-CP) fibers to meet the growing demand on high throughput protein chromatography. C-CP fibers are produces with a variety of polymers (polyester, polypropylene, nylon) through a melt-spin process in the Department of Material Science at Clemson University[26]. Traditionally, C-CP fibers have eight channels that run co-linearly for the entire length of the fiber[27]. This unique fiber morphology creates a network of parallel pseudo-open tubular columns tens of micrometers across when packed into a column[28]. These fibers have significantly higher surface areas than circular fibers of similar diameters, causing spontaneous wicking action[29]. This leads to favorable hydrodynamics as flow paths are oriented longitudinally leading to efficient fluid transport for significantly low column back pressure[30], and limiting band broadening caused by radial diffusion[31]. The high column permeability allows for operation with low-pressure solvent pumps or at high linear velocities. With traditional porous media the use of high velocities would lead to extensive C-term broadening, as defined by the Van Deemter equation[32]. This is not the case with C-CP fibers; the fibers have

the added benefit of being non-porous with regards to the biomarcomolecules which are being separated[33]. C-term broadening for non-porous surfaces is only limited by the transport kinetics of the analyte from the bulk flow to the solid-liquid interface, and adsorption kinetics at that interface[34]. Operation at high linear velocity causes the flow to become turbulent, which facilitates the transport of macromolecules to the solid-liquid interface[35]. The combination of the fluid transport characteristics and the mass transfer kinetics allows for high speed protein separations[36]. Protein separations have been accomplished on C-CP fibers using a variety of separation mechanisms including, reversed phase, ion-exchange[37], and hydrophobic interaction chromatography[38]. In all cases, employing high linear velocities with slow gradient rates yields the highest resolution[39].

The base chemistry of the various fiber materials has proven to be useful in a variety of works, as seen above, but the fiber base material is limited by what can be extruded into C-CP fibers. Due to this, extensive efforts have been taken to chemically modify the C-CP fiber surface to enhance the available surface chemistries[40-43]. Aside from direct covalent surface modification techniques the group has also uses hydrophobic adsorption on polypropylene fibers to affix specific ligands to the surface[44,45]. Of specific interest to this work is the development of Lipid Tethered Ligands (LTL) for surface modification. An LTL consists of a set of hydrophobic tails, a polar linker arm, and a reactive polar head group[46]. When exposed to a hydrophobic surface under aqueous

conditions the LTL adsorbs to the surface, anchoring the polar head groups to the surface. This methodology has been proven effective for the extraction of proteins from solution using an appropriate ligand affinity system[47]. LTL adsorption is stable under a wide array of solvent conditions, but can be desorbed from the surface with the inclusion of a non-polar solvent[48]. The development of a second generation LTL that is more stable and contributes a better surface population has since been developed[49].

In this thesis two different studies have been accomplished advancing the science developed with C-CP fibers. A new, wildly different generation of C-CP fibers has been developed which only has three larger more rigid channels. The goal of this study is to evaluate the new fiber with regards to parameter relevant to gradient protein separations, and achieve separation of a six-protein suite. The next study was designed to evaluate the potential for the application of the LTL modification modality on more a traditional polymeric hydrophobic chromatographic support. This includes loading condition optimization, LTL loading capacity and kinetics, quantification of ligand efficiency, and evaluation of LTL stability on the new support.

CHAPTER TWO

Dynamic Evaluation of New Capillary-Channeled Polymer (C-CP) Fiber Shape for Reversed Phase Protein Separations, and its Comparison to Traditional C-CP fibers

INTRODUCTION

Reversed phase (RP) chromatography is one of the most commonly used separation modes[50]. Championed by acyl-bonded silica resins[51], reversed phase chromatography is capable of separating analytes in complex mixtures based on hydrophobicity, the ability to participate in hydrogen bonding, and the extent of ionization[52]. One of the most significant areas of using reversed phase chromatography is applications in the biological sciences and the purification of bio-analytes. RP-HPLC has been used to separate DNA[53], nucleotide metabolites in blood sample[54], proteins in complex mixtures[55], and for peptide analysis[56], clearly demonstrating the methods universal role in the separation of biological analytes. Alkyl-silica micro-particulate stationary phases have delivered high separation efficiency, versatility, and reproducibility[57].

However alkyl-silica micro-particulate stationary phases are not without disadvantages. Most of the surface area in silica resins is inside the porous silica particles, leading to high binding capacities at the expense of diffusional band broadening. As chromatographers are pushed to develop ever greater column efficiencies, the size of the particles continue to decrease[58]. Decreasing particle

size produces ever greater back pressures, which has eventually led to the development of UHPLC[59,60]. In theory decreasing particle size is not a problem, but there is a large cost associated with higher back-pressures as the pumping systems require exponentially greater manufacturing and maintenance costs. Silica based phases are also known to not be stable under high pH conditions[61], or with prolonged exposure to phosphate buffers common to biological sciences[62]. These issues reduce column lifetime, increasing the chance to produce exposed ionizable silanol groups. There is an additional concern of specific surface areas for large molecules. Large biomolecules, such as proteins, have hydrodynamic radii on the same order of magnitude as the pores in porous silica, effectively leaving them unable to exploit majority of the particles surface area[63]. In response to these short comings stationary phases with superior chemical stability, mass transfer and hydrodynamic properties have been developed[64]. Historically monolith stationary phases have been on the forefront of this frontier. Monolith columns are based upon the polymerization monomers to create a through-pore network, allowing for the application of high flow rates at moderate back pressures[65].

Marcus and coworkers have been developing capillary-channeled polymer (C-CP) fibers as an alternative solution to the packed silica problems stated above. C-CP fiber columns consist of collinearly packed, multichanneled fibers. C-CP fibers are made through a melt extrusion process, with a specially shaped spinneret. Traditionally, C-CP fibers have been extruded with eight channels that

run the length of the fiber. In an attempt to exploit various surface chemistries, the fibers have been made from polypropylene, polyester, and nylon. The combination of the fiber structure and orientation minimizes flow restrictions, allowing the column to operate at extreme linear velocities without excessive system back pressures[66]. At high packing densities the fibers begin to interdigitate and form collinear channels that act similarly to open tubular columns[34] with regards to mass transfer and hydrodynamic properties. As would be expected in an open tubular format, C-CP fiber performs poorly in small molecule separations due to the low specific surface area[28] and limited porosity of the polymer fibers[33].

Alternatively, C-CP fibers have performed well for the separation of proteins. Proteins and other similarly large molecules are too big to diffuse into the stationary phase due to the limited porosity of the polymer fiber. Large molecules diffuse much slower than small molecules. As a result, porous stationary phases exhibit significant protein peak broadening due to the rates of diffusion in and out of the porous media to the bulk flow[67]. This effect is exacerbated by increasing linear velocity of the bulk flow. This effect is commonly known as C-term broadening, as described the Van Deemter equation. Both open tubular and C-CP fiber columns have limited porosity and can be considered non-porous in respect to larger protein molecules. Slow diffusion of proteins can cause serious bandspreading problems for large micro-channels and interparticle voids alike, as the protein in the bulk flow will not diffuse readily

from the bulk flow to the stationary phase. C-CP fibers are able to solve this problem by running at high linear velocities, resulting in turbulent flow conditions facilitating the interaction of the protein with the polymer surface[35]. C-CP fiber columns are able to operate at high flow rates, with improved mass transfer kinetics at those high flow rates. This combination of properties gives C-CP fibers potential for high throughput separations.

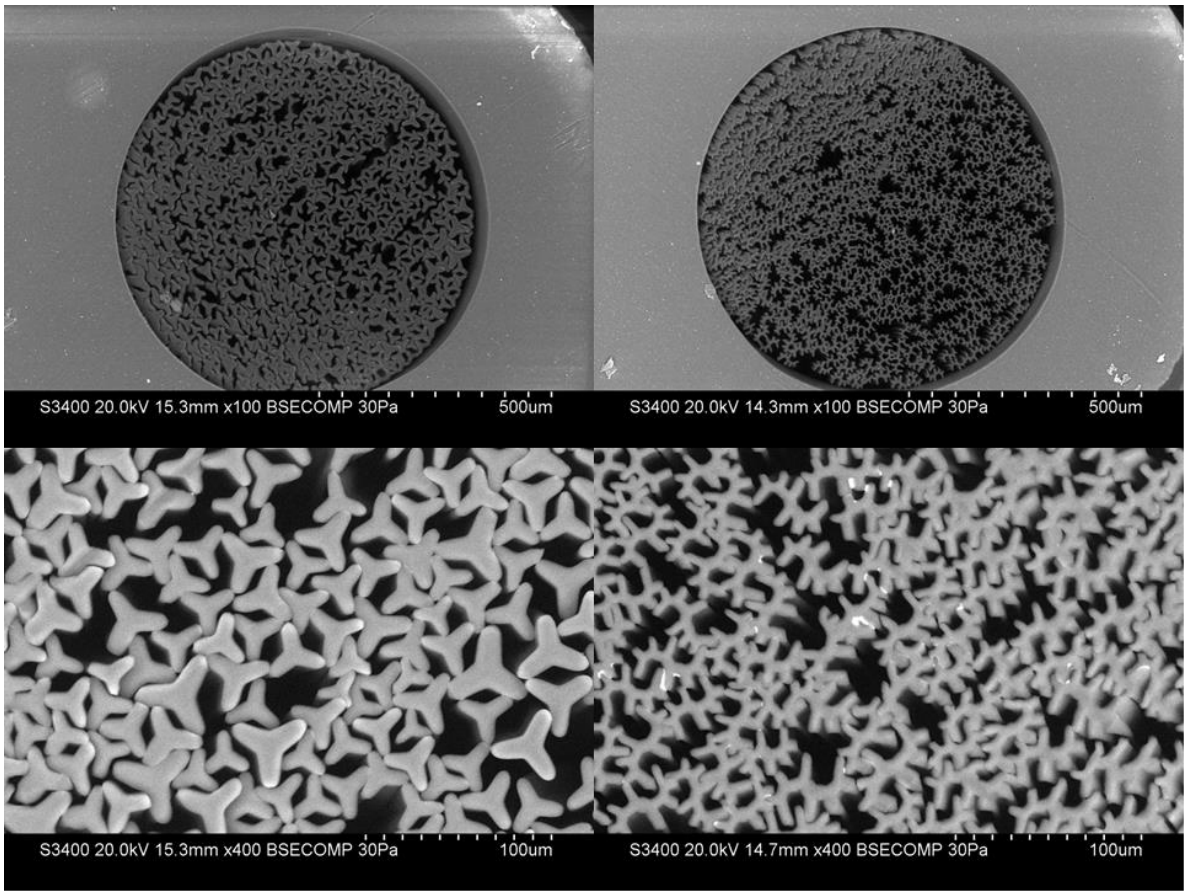

Figure 2.1 SEM images of C-CP fiber packed columns. PPY on the left was packed at ε_i=0.445 . PP4 on the right was packed at ε_i=0.638

As stated earlier, traditionally C-CP fibers have been extruded with eight channels that run the length of the fiber. Unfortunately these channels tend not to be uniform in size, and as a result are a source of column inefficiency. Over time, the eight channeled fiber extrusion process has been optimized to produce more uniform channels and smaller C-CP fibers. This work compares two fiber shapes, and the effects that the shape of the fiber have on the separation properties. The traditional eight-channeled fiber (denoted from this point onward as PP4) is compared to the new "Y" shaped fiber (denoted as PPY). **Figure 2.1** show SEM images of PPY and PP4 packed columns. It is clear that the "Y" shaped fiber is larger than the traditionally shaped fibers, having larger wide open channels as well as thicker channel walls. Both fibers have a problem with fiber to fiber variability, as some of the fibers are much larger than the others. As these problem fibers cannot be removed their impact cannot be evaluated. It is hypothesized that the "Y" shaped fiber will have a better packing uniformity as the variation of the channels on the fiber has been made insignificant. Comparison of the two shapes of fibers has been done under reversed phase conditions for protein separations. Reversed phase mode was chosen, as the use of the hydrophobic characteristics of C-CP fiber is currently the most widely exploited. The results of this study should provide useful insight in the production of next generation C-CP fibers for high throughput protein separations.

EXPERIMENTAL

Materials

HPLC grade Acetonitrile and methanol were purchased from EMD Millipore. Milli-Q water (18.2 MΩ-cm) was purified using a Millipore water purification system. Bovine serum albumin (BSA), ribonuclease A (bovine pancreas), cytochrome C (Bovine heart), transferrin (human), lysozyme (human), α-chymotrypsinogen (bovine pancreas) were all purchased from Sigma-Aldrich.

Column Construction

Polypropylene C-CP fibers were manufactured in the School of Material Science and Engineering at Clemson University. The Fibers were extruded with the traditional eight channels and in a new three channel "Y" shaped format. Polyether ether ketone (PEEK) tubing was purchased from Cole-Parmer at 0.76mm internal diameter. Columns were packed with C-CP fiber using previously described methods[44]. Fibers were packed in columns at different packing densities to produce columns with different interstitial fraction. Packed C-CP fiber columns were fitted with PEEK unions (VWR International)

The C-CP fiber columns were mounted on a Dionex Ultimate 3000 HPLC system (LPG-3400SD Quaternary pump, MWD-3000 UV–Vis absorbance detector (Thermo Fisher Scientific Inc., Sunnyvale, CA)) and washed with acetonitrile and deionized water until a stable baseline was observed at 216 nm. Scanning electron microscopy was used to examine the new fiber and the packing uniformity at varying interstitial fractions. A field emission scanning electron

microscope (Hitachi, SU4800, Japan) was set to variable pressure mode at 30 Pa, and the accelerating voltage was set to 20 kV.

Method

Data for the Van Deemter study was collected using two markers. The uracil marker was used with a mobile phase of 5% acetonitrile water with 0.1% TFA. The BSA marker was used with a mobile phase of 50% acetonitrile water with 0.1% TFA. The data in Fig 3 was collected at 25, 50, and 75% acetonitrile water with 0.1% TFA. The study included measurements of only the pumping system and the pumping system plus the empty PEEK column. The resolution data was calculated using data collected from Chromeleon 6.8 software for the gradient separation of ribonuclease A and transferrin. All Data was collected in triplicate for each flowrate evaluated, and columns of different interstitial fractions were used.

Gradient and flowrates were optimized using a 20 µl injection of a four-protein suite (ribonuclease A, cytochrome C, transferrin, and BSA). Optimized conditions were applied to a six-protein suite which contained lysozyme and α-chymotrypsinogen, in addition to the above described four-protein suite. The stock solutions were prepared with 100 ppm of each protein in water the day of the analysis. Injection volume for the six-protein separations were limited to 5 µl to avoid column overloading. Each separation was completed twenty times on each column; runs 1, 10, and 20 are reported. Additional columns were made with the same parameters as two best performing columns. The six-protein suite

was then separated again using the new columns and the first separation on each column was compared. Column permeability was determined using Darcy's Law for acetonitrile, water and methanol. The permeability was calculated for ten different flowrates ranging from 0.1-1.0 ml/min, and the results were averaged.

RESULTS AND DISCUSSION

The most common method to determine chromatography column efficiently is to calculate the number of theoretical plates for a given column. Columns that have a higher number of theoretical plates are considered to be more efficient. Columns with high plate numbers will have sharper peaks than a column with fewer plates at the same retention time. Plate number is defined as

$N = 16(t_r/w)^2$ (1)

where N is the number of theoretical plates, t_r is the retention time, and w is the width of the peak. Plate number (N) is more commonly calculated by

$N = 5.545(t_r/w_{0.5})^2$ (2)

where $w_{0.5}$ is defined as the peak width at half height. This equation was adopted due to the large amount of uncertainty in determining the actual width of the peak. Both of these equations assume that the peak is Gaussian, and the further the peak shape drifts from Gaussian the less reliable the plate number data becomes.

Increases in plate height can be attributed to zone broadening. Zone broadening can be impacted by three different subsets of peak broadening,

caused from variation in average flow path, longitudinal broadening, and mass transfer kinetics. These three sub classifications of peak broadening are described in the Van Deemter equation.

$$H = A + {}^{B}/_{u} + Cu \quad (3)$$

H is defined as the height of each theoretical plate. It is calculated by the quotient of the column length by the number of theoretical plates. u is defined as the linear velocity of the mobile phase. The A-term represents all of the factors that lead to variations in flow paths. The effects of A-term broadening are minimized by increasing packing uniformity. B-term broadening is longitudinal diffusional broadening. Molecules in solution diffuse from areas of high concentration to areas of low concentration. This phenomenon occurs in chromatographic systems as the sample plug broadens as it diffuses to areas of lower concentration. This process takes time, so then longer the sample is in the column the more longitudinal broadening will take effect. As a result B-term broadening is inversely proportional to the linear velocity of the mobile phase. When analytes diffuse into a porous media they leave the bulk flow of the column. Inside the porous media the analytes experience flow stagnation, or simply areas of retarded flow rate as most of the mobile phase flows around the porous media. As some analyte spends more time in the porous media the rest of the analyte is moving along the column in the bulk flow. This causes the analyte molecules in the porous media to be left behind, increasing C-term broadening[68].

Traditionally shaped (eight channeled) C-CP fibers were found to have optimum packing uniformity at an interstitial fraction of $\varepsilon_i \approx 0.63$[31]; this finding has been confirmed over a few separate studies including this one. The actual ε_i was determined for each column using the retention time of an unretained uracil injection, and calculated using equation 4.

$$\varepsilon_i = \frac{F(t_r - t_0)}{V_c} \quad (4)$$

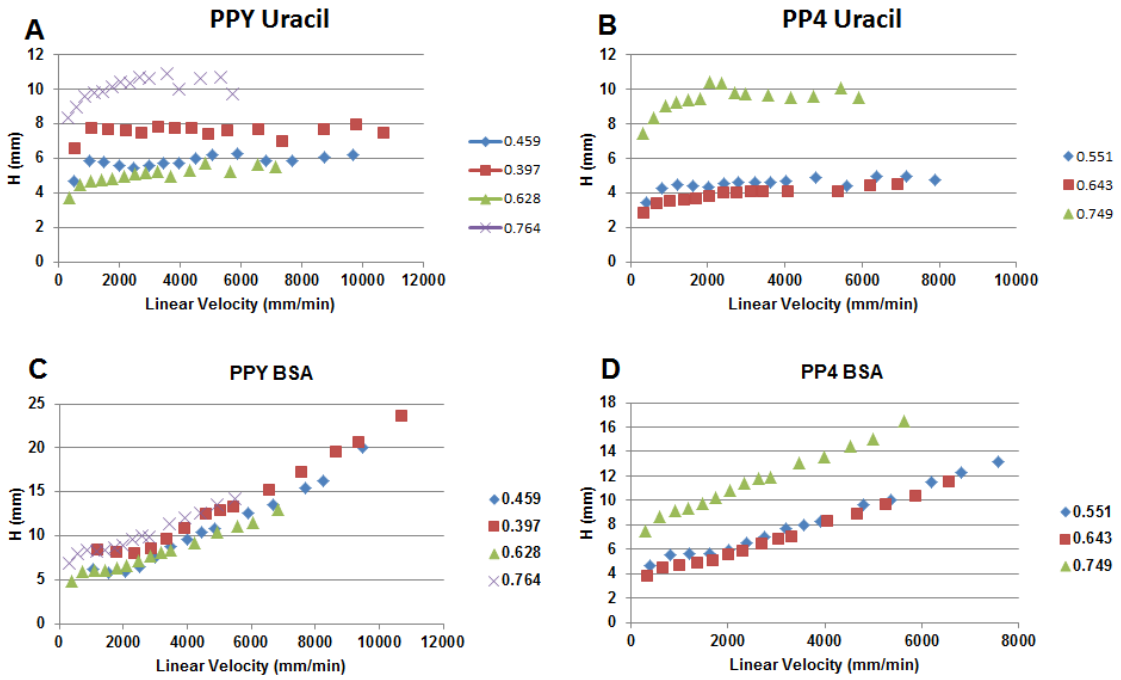

Figure 2.2 Each Van Deemter plot was generated for one of the fiber types using one of the markers. Markers included uracil at 5% Acetonitrile water with 0.1% TFA, and bovine serum albumin at 50% acetonitrile water with 0.1% TFA. All analysis were completed on 30cm microbore columns.

Where F is the mobile phase flow rate, t_r is the retention time for the uracil injection on the column, t_0 is the retention time for the uracil injection without the column, and V_c is the volume of the empty column.

In this study the column efficiently of two differently shaped polypropylene C-CP fibers was determined. The fourth generation of the traditionally shaped (eight channeled) C-CP fiber was compared to the newly developed "Y" shaped fiber. **Figure 2.2** compares four different sets of Van Deemter plots, using both

bovine serum albumin and uracil as unretained markers. Each plot contains graphs for each different interstitial fraction. It can be seen, **Figure 2.2 b,d**, that the previous results relating to traditionally shaped C-CP fiber have been confirmed. With both markers, the ε_i=0.643 column vastly outperformed the ε_i=0.749 column, while performing marginally better than the tighter ε_i=0.551 column. As the column is packed tighter, the standard deviation of the channel diameter decreases. The tighter packing (0.0749 IF to 0.643 IF) causes interdigitating of the C-CP fibers leading to a higher degree of channel uniformity. Once the fiber is packed too densely, the channels can start to collapse and some can be completely occluded.

For the new PPY C-CP fiber this pattern no longer holds as strongly. The two markers produce slightly different results. While the uracil marker on PPY shows similar results when compared to the PP4 trend, the BSA marker does not confirm that $\varepsilon_i \approx 0.63$ is the best packing density for the PPY fiber. The uracil marker on PPY does not suggest that as the interstitial fraction deviates from $\varepsilon_i \approx 0.63$, the efficiently of the column decrease. This is what would be expected if the new "Y" fiber was to conform to the traditional trend. The BSA marker

shows significant overlap of the ε_i=0.628 and the ε_i=0.459 columns. Due to the discontinuity in the results, the best PPY interstitial fraction will have to be determined using a supporting experiment. It is important to point out that for each marker the PP4 column consistently performed better than the PPY columns, having marginally smaller plate heights.

As discussed above C-term broadening is a major concern. For both the PPY and PP4 fiber columns the uracil marker confirms negligible C-term broadening, even at exceedingly high linear velocities. This means that C-CP fiber columns can maintain efficient performance at high linear velocities. Unlike the uracil marker, the BSA marker seems to have a slight slope that would be indicative of C-term broadening. Originally troubling, this minor slope would appear flat when compared most monoliths operating at the same linear velocity[69].

The seeming existence of C-term broadening with one marker but not the other can be used to glean some information about the system. For example, if the small uracil marker had C-term broadening but the BSA marker did not, it would indicate that the polypropylene fiber is semi porous to the uracil . In this case however, the larger molecule seems to be exhibiting minor C-term like broadening while the smaller molecule is not. It would suggest that broadening is not due to kinetic concerns, but rather caused by some sort of weak interaction with the stationary phase or system. If a chemical interaction is causing slight

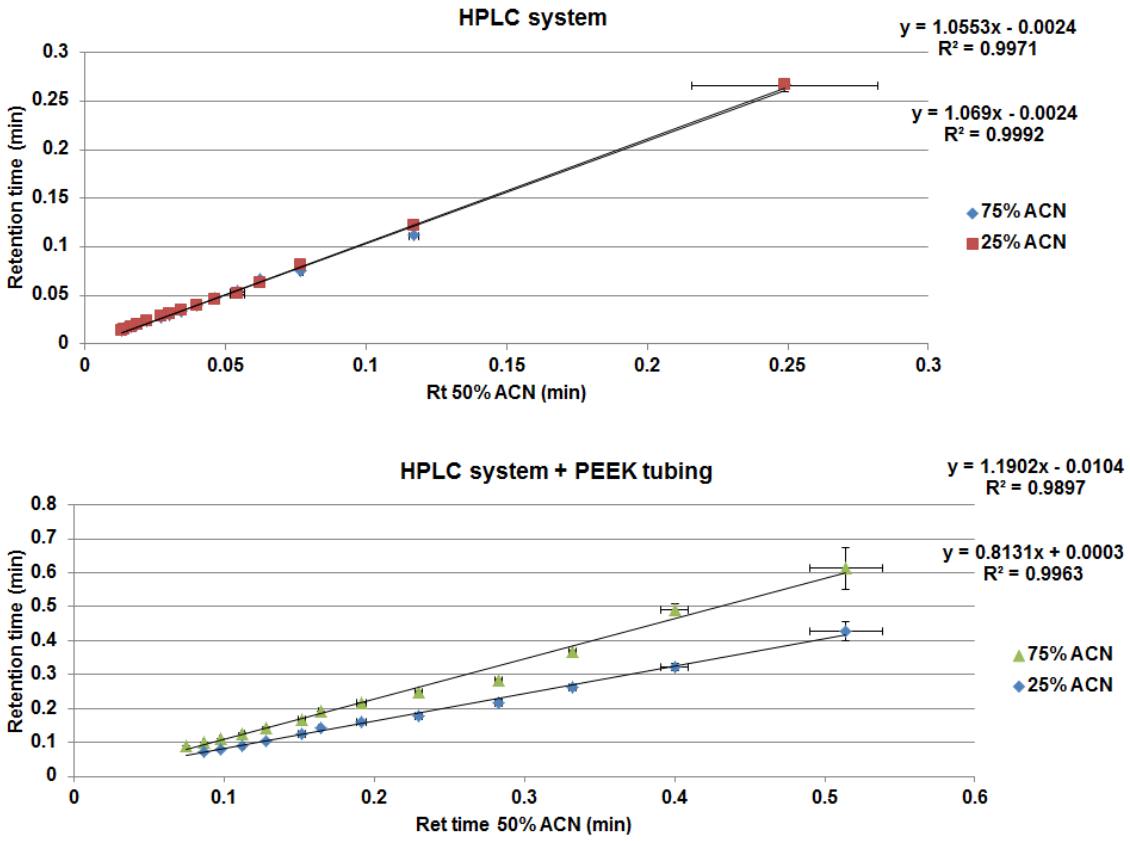

Figure 2.3 Comparative study for the retention of BSA under different solvent conditions. Each plot contains the retention time data from three graphs of flow rate vs retention time using different solvent compositions. In all evaluations the same sets of flow rates were used 0.1, 0.2, 0.3, 0.4, 0.5, 0.6, 0.7, 0.8, 0.9, 1.0, 1.2, 1.4, 1.6, 1.8, 2.0 ml/min. TOP: The retention time of BSA for the HPLC system at 50% ACN at different flow rates vs retention time of BSA for the HPLC system at 25% and 75% ACN . BOTTOM: The retention time of BSA for the HPLC system with the addition of 30cm of empty PEEK tubing at 50% ACN at different flow rates vs retention time of BSA for the HPLC system at 25% and 75% ACN.

broadening of the BSA marker, then the retention time of the BSA peak will change with solvent condition. The original study with the BSA marker was run under elution conditions for BSA, 50% ACN/water with 0.1% TFA. In order to rule out the system, the retention time of BSA was monitored on the HPLC without column, and with an empty PEEK microbore column at different flow

rates. This was completed at 25%, 50%, and 75% ACN/water mobile phases with 0.1% TFA. If there are no chemical interactions, then plotting the data against each other should produce a straight line with a slope of 1 and a y-intercept of 0. When this study was performed on the HPLC system (**Figure 2.3a**) alone two nearly identical lines were formed that behaved exactly as predicted if no chemical interaction was present. This result can be contrasted with the result from the system plus empty column (**Figure 2.3b**). The slopes of the two lines in **Figure 2.3b** deviate from 1 by approximately 0.19. It can be seen that as the ACN concentration in the mobile phase increase, so does the retention of BSA on the PEEK tubing. This means that the PEEK microbore tubing used to make C-CP fiber columns is at least partially responsible for the non-ideal behavior of the BSA marker. In an attempt to isolate the effects from the polypropylene C-CP stationary phase from that of the PEEK tubing, FEP tubing was evaluated instead. Unfortunately, the FEP tubing also had a chemical interaction with the BSA and as a result we were unable to isolate the polypropylene fiber effects.

Effect of linear velocity, packing density, and fiber shape on resolution

Resolution is one of the most important characteristics in any separation. In order to get more information on the best packing density the resolution of two peaks were monitored at different flow rates for a set gradient, for columns with different interstitial fractions. As the most promising application of C-CP fibers is in the purification of proteins, ribonuclease A and transferrin were separated

using a previously published gradient[70]. The resolution of these two peaks was calculated using equation 5.

$$R_s = \frac{2(t_2 - t_1)}{w_2 + w_1} \quad (5)$$

where R_s is the resolution, $t_{1\ or\ 2}$ is the retention time, $w_{1\ or\ 2}$ is the width of the peak. The flow rate was plotted against the resolution for both PP4 and PPY.

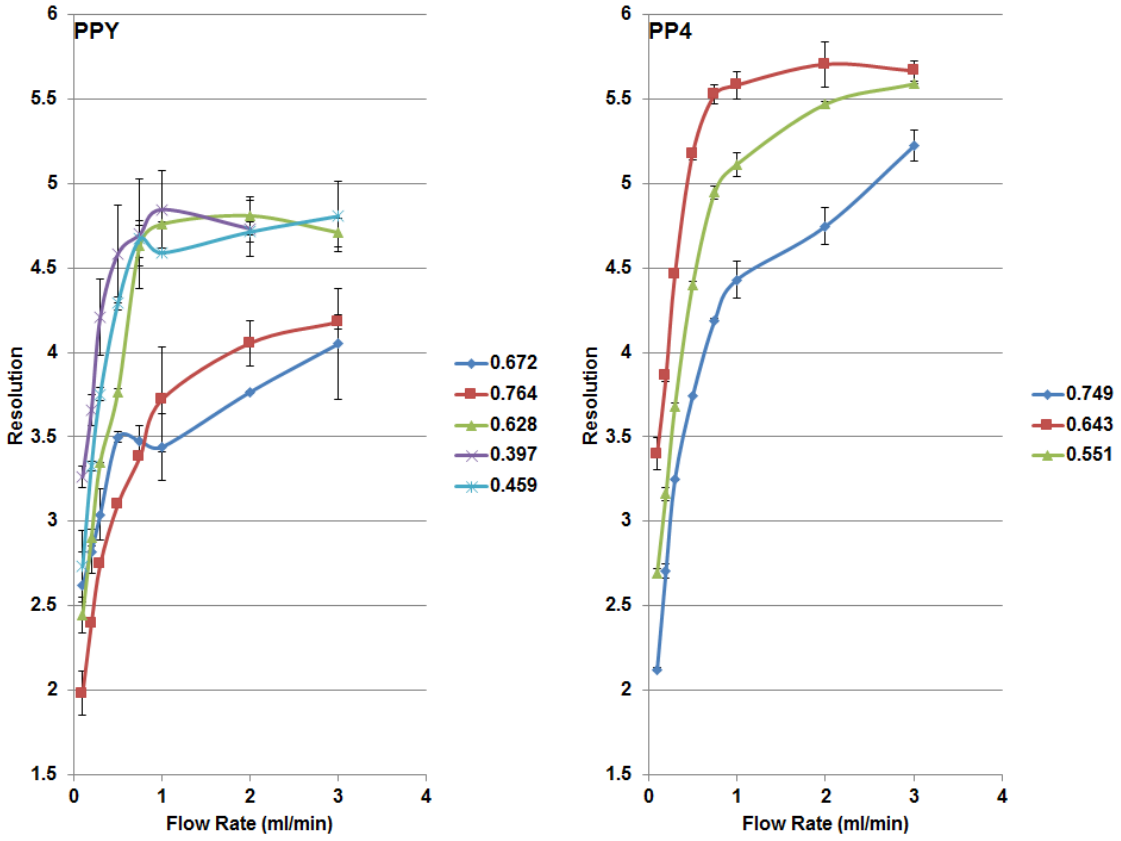

Figure 2.4 Plots of resolution vs flow rate for the gradient separation of ribonuclease A and transferrin for both PPY and PP4 fiber columns. Each curve represents a column at a different interstitial fraction.

Figure 3 clearly shows that $\varepsilon_i \approx 0.63$ is still the optimal interstitial fraction for PP4, as the resolution is higher for ε_i =0.643 across the board. It is noteworthy that all

of the PP4 curves seem to be converging on a limit. This suggests that the resolution gains from increasing the flowrate will eventually approach 0. When examining the PPY data, it is clear that the tighter columns will yield better resolution. When examining the two interstitial fractions that were previously identified as the most efficient by the Van Deemter plots, it is clear that above 1 ml/min there is no significant difference between the resolution measurements.

When comparing the results of the Van Deemter experiment to that of the resolution experiment, it could be perceived as slightly contradictory. Even though both agree on optimal packing density for both columns, the data suggest large disparities in optimal flow rates. The Van Deemter data suggests that marginal improvements would be seen at smaller flowrates, whereas the resolution data suggests that operating below 1 ml/min will drastically decrease resolution. This difference is due to the presence of adsorption/desorption interactions in the gradient study. C-CP fibers are known for having no significant amount of C-term broadening for large analytes. The minute changes in uracil plate height at high linear velocities, as seen in **Figure 2.2**, are caused by peak asymmetry at high flowrates, but more importantly it confirms that exceedingly high linear velocities will not harm the overall separation. When operating in gradient mode the high linear velocities continue to lead to greater performance due to the rapid elution of analytes from the column post desorption. As reversed phase separations on polypropylene C-CP fiber are not

isocratic, the results of the gradient resolution will dictate optimal flow rate conditions.

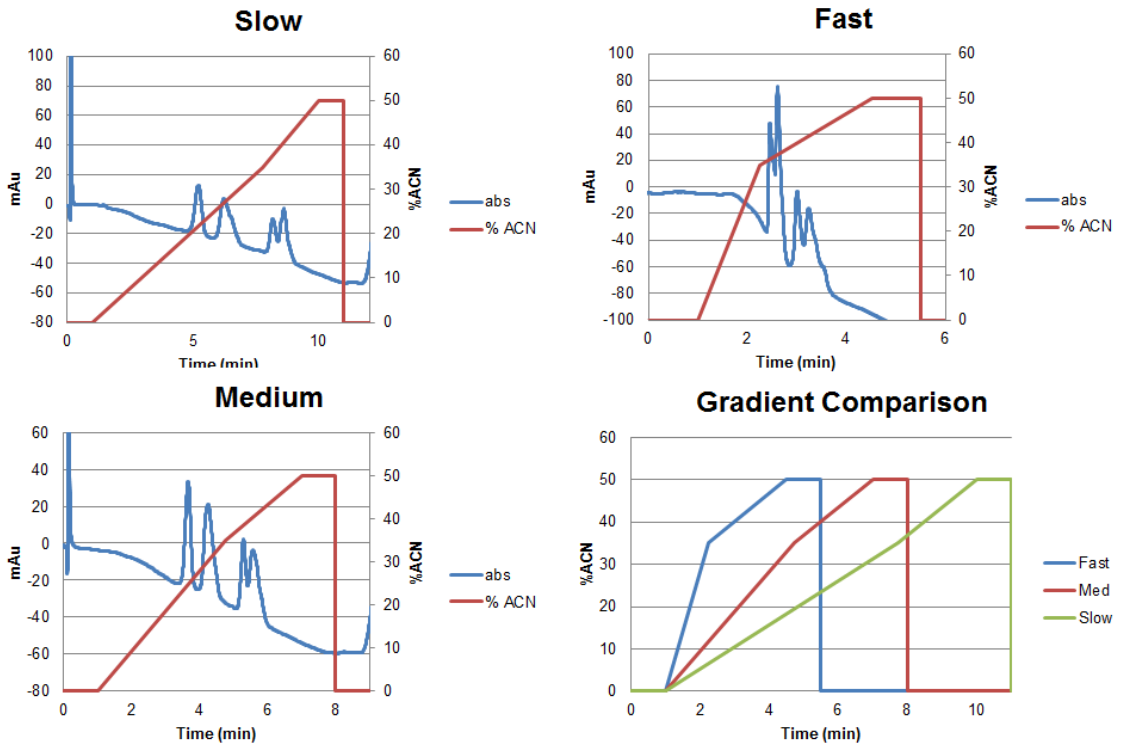

Figure 2.5 Sample of the PPY gradient rate optimization with the separations of four proteins: ribonuclease A, cytochrome C, transferrin, bovine serum albumin. **A**: slow gradient starting at 1 minute the %ACN is increased to 35% at 7.75 minutes, and increases to 50% by 10.3 minutes. **B**: medium gradient starting at 1 minute the %ACN is increased to 35% at 4.75 minutes, and increases to 50% by 7 minutes. **C**: fast gradient starting at 1 minute the %ACN is increased to 35% at 2.25 minutes, and increases to 50% by 4.5 minutes.

Reversed phase separations of four proteins on C-CP fibers were optimized and evaluated. Four variables control the quality of a protein separation on C-CP fiber columns: packing density, linear velocity, gradient

slope, and identity of organic modifier. Packing density is expressed as the interstitial fraction of the column in question. In order to gain further understanding of the impact of packing density, linear velocity, and gradient slope were optimized. Both fibers in question are made of the same material, and as a result are going to have the same chemical selectivity for each protein. **Figure 2.5** shows a sample of the optimization work for the gradient. A gradient that is too steep will lead to poor resolution between proteins. In contrast, slow gradients are seen to cause peak broadening and deteriorate peak shape. Both of these observations suggest that each protein does not simply elute completely from the stationary phase once a specific solvent composition is reached. This would explain why broadening is observed for the protein peaks under slower gradient rates. If only solvent composition was a factor, then the resolution at different slopes would be maintained. This does not seem to be the case as the ribonuclease A and cytochrome C peaks begin to merge into one another, indicating that the desorption process is also kinetically limited. As a result the gradient in **Figure 4B** was selected for optimization. Using the gradient selected, the flow rate was varied from 1.5-3 ml/min. Marginal gains were observed with increases in linear velocity. In previous work it was determined that as the linear velocity, and thus the shear rate, increases the C-CP fiber stationary phase will require less organic modifier to cause protein elution[38]. The data collected in this experiment does not follow the same trend as previously reported. In that work linear velocities of much less than 2000 mm/min were used for the analysis.

Linear velocities as high as 10700 mm/min for PPY and 7000 mm/min for PP4 were used in this work. This seems to indicate that the selectivity differences observed due to changes in linear velocity previously published stop occurring or become negligible at exceedingly high linear velocities. Unfortunately, the PEEK microbore columns packed to make the C-CP fiber columns are liable to failure (blow out of the ferrule) at pressures above 2500 psi. This was not a problem for the columns at $\varepsilon_i \approx 0.63$, but became far more prevalent for $\varepsilon_i = 0.445$ PPY columns. Due to this mechanical problem and the insignificant improvements in resolution, the operational flowrate was chosen to be 2 ml/min. Operating C-CP fiber columns at such large linear velocities confirms that C-CP fibers have no C-term broadening.

Using the optimized conditions a solution of six proteins was analyzed. The solution contained 100ppm of ribonuclease A, cytochrome C, lysozyme, transferrin, bovine serum albumin, and α-chymotrypsinogen A. Three different columns were evaluated PPY $\varepsilon_i = 0.445$ and $\varepsilon_i = 0.628$, and PP4 $\varepsilon_i = 0.638$. When examining two columns of similar interstitial fraction (**Figure 5**) it is clear to see that both peak shape and column efficiency is superior on PP4 when compared to PPY. PPY has base line separated ribonuclease A, cytochrome C, and lysozyme. In comparison the only proteins not resolved by PP4 are transferrin and bovine serum albumin. The separation achieved using the $\varepsilon_i = 0.445$ PPY column is superior to that of the PP4 column, resolving all six proteins. This result is surprising since every other evaluation has led to the

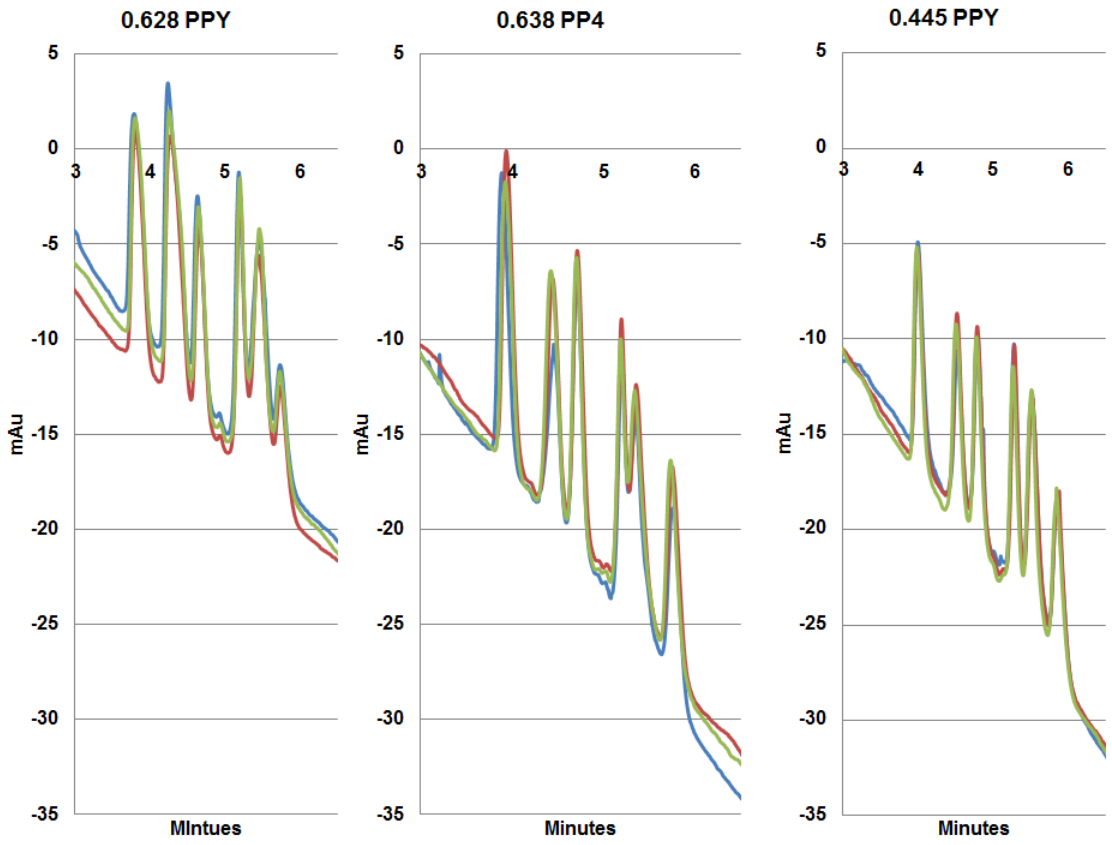

Figure 2.6 Chromatograms of a six protein reversed phase separation with the elution order: ribonuclease A, cytochrome C, lysozyme, transferrin, bovine serum albumin, alpha chymotrypsinogen. Replicate separations were done to show column robustness, plotted are the first, tenth and twentieth separation. The applied gradient is identical to the gradient in figure 5B.

conclusion that PP4 was superior. PP4 clearly has a better packing uniformity leading to better resolution and lower plate heights than PPY. The explanation for this is the acceptable, while not superior, packing uniformity of the PPY fibers at higher packing densities. The simple fact that C-CP fibers have no C-term broadening implies that the only limitation to the mass transfer kinetics is the rate of desorption from the stationary phase. As the mobile phase changes with time, faster flowrates will cause faster desorption and will result in sharper peaks. At

the same flow rate of 2 ml/min, the ε_i =0.445 PPY column has a linear velocity of ~9500 mm/min in comparison to the ε_i =0.643 PP4 column that has a linear velocity of only ~6500 mm/min. That is a 46% increase in linear velocity over the comparable PP4 column. Unlike the PPY fiber, PP4 does not operate nearly as well at higher packing densities. This is most likely due to channel collapse of the eight channeled fiber creating more variation in the average channel diameter. The channels on PPY are much larger and much more resistant to channel collapse allowing for higher packing densities without sacrificing packing uniformity. It is clear that the large increase in linear velocity was able to overcome the packing uniformity problems of PPY.

Column Permeability of PPY and PP4 C-CP fiber columns

The permeability of the two best performing columns was calculated for the three most common solvents in reversed phase chromatography (**Figure 2.7**). The permeability was calculated according to Darcy's law[71].

$B^o = \frac{\eta * L * Q}{A * \Delta P}$ (6)

Mobile Phase	Viscosity (mPa*s)	Relative Polarity	Average Permeability (x$10^{-10}$$m^2$)	
			0.445 PPY	0.638 PP4
Acetonitrile	0.37	0.46	1.37±0.03	1.82±0.02
Water	0.89	1.00	1.35±0.03	1.83±0.06
Methanol	0.54	0.54	1.21±0.04	1.66±0.02

Table 2.1 Reports average permeability with standard deviation for both the best performing PPY and PP4 column, as well as viscosity, relative polarity of each solvent used.

B^o is the permeability, η is the viscosity of the mobile phase, L is the length of the column, Q is the flow rate, A is the cross sectional area, ΔP is the back

pressure of the system. Table 1 contains the specific permeability of the two columns for each mobile phase. There is no surprise that the PPY fiber column has a lower specific permeability than the PP4 column, due to the higher packing density. Both of the permeability measurements are vastly superior to most monolith columns, which have permeability measurements 10000-100000x smaller than C-CP fibers[72].

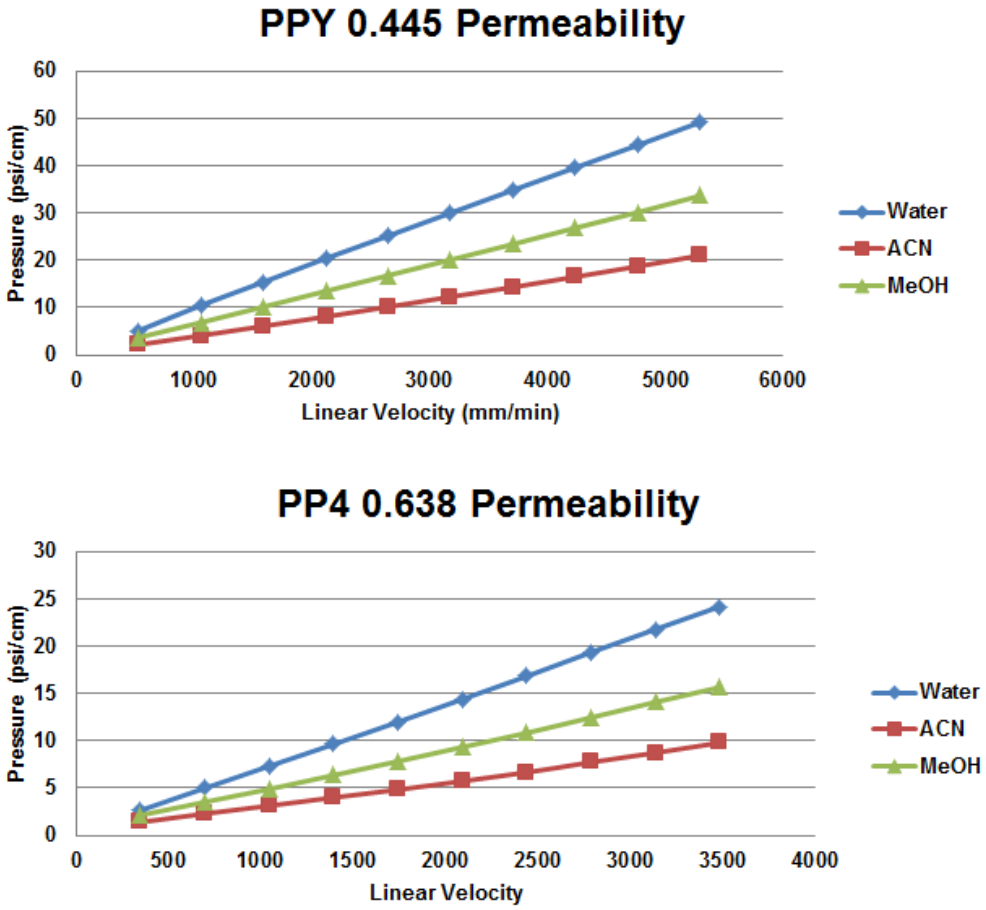

Figure 2.7 The back pressure of the system was monitored from 0.1-1 ml/min for methanol, acetonitrile, and water. From this data column permeability was calculated using Darcy's Law, and reported for each solvent in Table 2.1.

Column reproducibility is a major concern for any column characterization. Every column constructed is going to be different, but to provide reliable results

requires those differences to be minimal. Three separate columns for each fiber type were constructed and used to separate the out six proteins previously used. When examining **Figure 2.8** it is clear that the column to column variability is smaller for PP4. This is easily understood because it is packed looser, and relies more on the individual fiber than upon interdigitating to form channels.

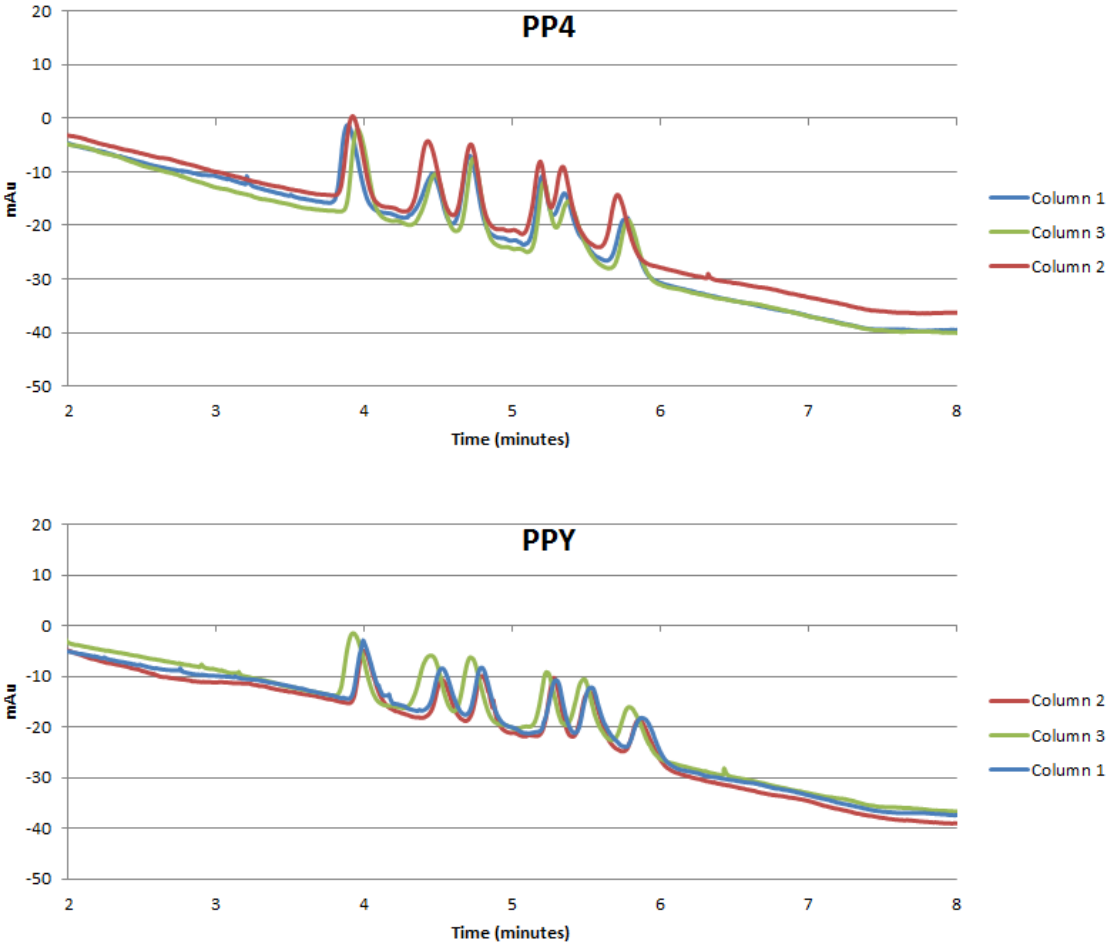

Figure 2.8 PPY and PP4 columns were constructed using optimal parameters determined in this work. Column to column variability was evaluated by examining how the separation of the six protein suite used in figure 6 changes from column to column.

The PPY fiber is also packed tighter leading to fiber crowding and changes in flow path that cannot be reproducibly accounted for. The stability of individual PPY and PP4 columns seems to be acceptable with minimal changes to the chromatogram over many replicate separations as seen in figure 4.

PARTIAL CONCLUSIONS

Two differently shaped C-CP fibers, PPY and PP4, have been evaluated to determine the potential of the "Y" shaped fiber. For both fibers the column efficiency was determined for a variety of interstitial fractions using two separate markers. Smaller plate heights were found for PP4 columns. Both fibers exhibited excellent mass transfer kinetics, which is indicates having a lack of C-term broadening even at exceedingly high linear velocities. The results for PP4 matched pervious results confirming that $\varepsilon_i \approx 0.63$ is the best packing density. The Van Deemter data suggests that, like PP4, over packing a column will lead to greater peak broadening , but at much higher packing densities. The Van Deemter data was inconclusive in determining the optimum packing density for PPY. The optimum packing density for PPY was not determined until each column was evaluated, under optimized conditions, by separating the largest protein suite ever published on unmodified C-CP fibers. The Resolution and peak shape between all peaks for $\varepsilon_i = 0.445$ was superior to that of the $\varepsilon_i = 0.628$ PPY columns. The protein separation on the $\varepsilon_i = 0.445$ column was

surprisingly better than the $\varepsilon_i = 0.638$ PP4 column, which performed better for column efficiency and resolution.

This study will allow for the development of superior next generation fibers. C-CP stationary phases are able to capitalize on the use of high linear velocities, due non-existent C-term broadening to produce a unique stationary phase. The use of high flowrates and short separation times indicates potential for high throughput reversed phase protein separations. When examining the size of the fiber it is clear that PPY is larger, with thicker walls, when compared to PP4. At traditionally optimal packing density, PP4 starts to interdigitate without channel collapse or occlusion leading to a better bed uniformity. The larger PPY fiber performs worse due to poor packing uniformity, attributed to the larger channels and the thicker channel walls. The PPY fiber shows promise at higher packing densities where the channel collapse does not occur. The higher packing densities of the PPY columns allows for operation at linear velocities great than 3000mm/min more than PP4 columns. With no C-term broadening present, operation at higher linear velocities causes superior separations by increasing column efficiency. It is clear that smaller C-CP fibers are the key to producing better performing chromatography columns. Smaller C-CP fiber, regardless of traditionally or “Y” shaped, will lead to superior packing as the variation in the microchannel decreases. Smaller fiber would also allow for tighter packing, which would increase the linear velocity on the column, and has been shown in this work to produce superior separations. General fiber to fiber

uniformity is clearly a problem, but its influence can only be determined post extrusion optimization. The real limitation is the spinneret tip used in the melt extrusion process. As long as that can be made smaller, then reversed phase separations on C-CP fibers can continue to advance.

CHAPTER THREE

Modification of Polystyrene-Divinylbenzene Resin with Lipid Tethered Ligands for Affinity Based Protein Separations

INTRODUCTION

The practical expansion of high performance liquid chromatography (HPLC) was facilitated by the parallel development of microparticulate silica synthesis technologies and the corresponding development of facile surface modification chemistries [50]. Indeed, the development of diverse silica support phases continues, as witnessed in the introduction of the highly porous 1.2 μm diameter silica particles that are the heart of ultra-performance liquid chromatography (UPLC) and the rebirth of poroshell-type phases [73-76]. The microporous silica packing materials are optimum for small molecule separations by virtue of their high phase ratios, short diffusion distances, and high packing uniformity, but fall short in the realm of protein and bio-macromolecule separations. The hydrodynamic radii of proteins and large macromolecules are of the same order of magnitude of the pores in microporous silica, leaving them unable to exploit the majority of the surface area of the stationary phase [77]. Silica support phases tend to degrade above pH 7, depending on the stationary phase makeup [78], while biological specimens are normally stored in/prepared in buffers, one of the most common being phosphate buffered saline, which is typically prepared at a slightly basic pH. An additional concern of the buffer for silica stationary phases as the stability erodes with long term exposure to phosphate

buffer, greatly reducing column lifetime [79]. One further complication is caused by the fact that residual surface silanol groups are deprotonated in the pH range of 4-7, imparting ion-exchange characteristic to the silica resin [80]. These fundamental issues have led to the preponderance of polymer-based support/stationary phases for biomolecule separations.

Early protein and biopolymer separations were typically performed using modified polysaccharides for size exclusion and ion-exchange chromatography [81,82]. Agarose gels are permeable to large molecules due to the macroporous structure. Though agarose gels can be easily modified, the porosity tends to change with the solvent conditions, a problem that is exacerbated in gradient separations. In addition, the gel matrix is not stable under elevated pressures [83]. Based on its chemical attributes, polystyrene divinylbenzene (PS-DVB) is the most commonly used polymer stationary phase [84]. PS-DVB does not have the same mechanical stability problems as the carbohydrate-based polymer stationary phases, being stable at pressures up to 5000 psi [80]. PS-DVB is generally stable across the entire aqueous pH range, important as strongly basic conditions are often employed in the cleaning and regeneration of columns for biomacromolecule separations. In terms of separation mode versatility, the phase is extremely hydrophobic, and the surface must be modified extensively before anything other than a reversed phase separation can be affected.

The derivatization of PS-DVB is more complex than its silica counterpart, but does not run the added risk of losing functionality by post-modification

hydrolysis. Boiling the resin in fuming sulfuric acid was originally used to add sulfonate functional groups to the surface for cation exchange [80]. Less extreme reactions have been developed using glacial acetic acid and concentrated sulfuric acid to impart surface sulfonation [85]. Polystyrene resins are commonly modified with 1-chloromethyl ether using a Friedel-Crafts reaction, to create chloromethyl-derivitized resins for solid phase peptide synthesis [86]. More recently, Zhao et al. modified chloromethyl PS-DVB resin with the imidazonium functinality, which is normally employed for immobilized metal affinity chromatography (IMAC) [87]. The use of a simple hydrophobic adsorption mechanism has previously been used to facilitate polyvinyl alcohol cross-linking on PS-DVB resin [88-90]. Polyvinyl alcohol can be anchored to the surface via hydrophobic adsorption, and then subsequently cross-linked for mechanical stability and further derivatization. In practice, a second level of surface modification of the support is then necessary to impart greater selectivity to PS-DVB phases, for example the addition of affinity ligands. In these cases affinity ligands can be covalently attached to the surface of the resin by exploiting alcohol [91], imidazole [87], or other reactive functional groups.

The demand for high-selectivity purification continues to increase as the downstream possessing steps involved in production/isolation of protein therapeutics can account for as much as 80% of manufacturing costs [92]. Demands for chemical purity must be complemented in terms of the throughput and overall yield of the process [93,94]. To this end, the development of

high-selectivity capture chemistries must be augmented by implementation on phases having high production efficiency. This laboratory has placed recent efforts into both the throughput *and* purity aspects of protein separations. Specifically, the group has introduced the use of capillary-channeled polymer (C-CP) fibers as stationary phases for analytical and preparative protein separations [30,95-101]. In an effort to develop a generalized methodology to impart selectivity, the concept of lipid tethered ligands (LTL) as a means of anchoring selective functionalities to a hydrophobic, polypropylene, C-CP fiber surface has been developed [48,102-104]. In this format, the hydrophobic acyl chains of the lipid adsorb to the fiber surface. Steric control and a level of near-surface hydrophilicity can be imparted through the inclusion of a polyethylene glycol (PEG) spacer, in first generation LTLs. In second generation LTLs the PEG spacer has been reduced to a single monomer unit to allow for a greater surface population. The stability of the adsorbed LTL on the polymer surface was also shown to increase in the second generation LTL. Finally, chemical selectivity is affected through the covalent attachment of selective R-groups. The basic chemical structure of the LTLs is presented in **Figure 3.1**, along with the structures of the R-groups employed here, fluorescein and biotin. The strong physical adsorption of the aliphatic lipid tails anchors the affinity ligand to the hydrophobic polypropylene fiber, and produces a stable platform for protein separations [48,103]. Selective protein capture from cell lysate has been achieved and the robustness of this system has been demonstrated [103].

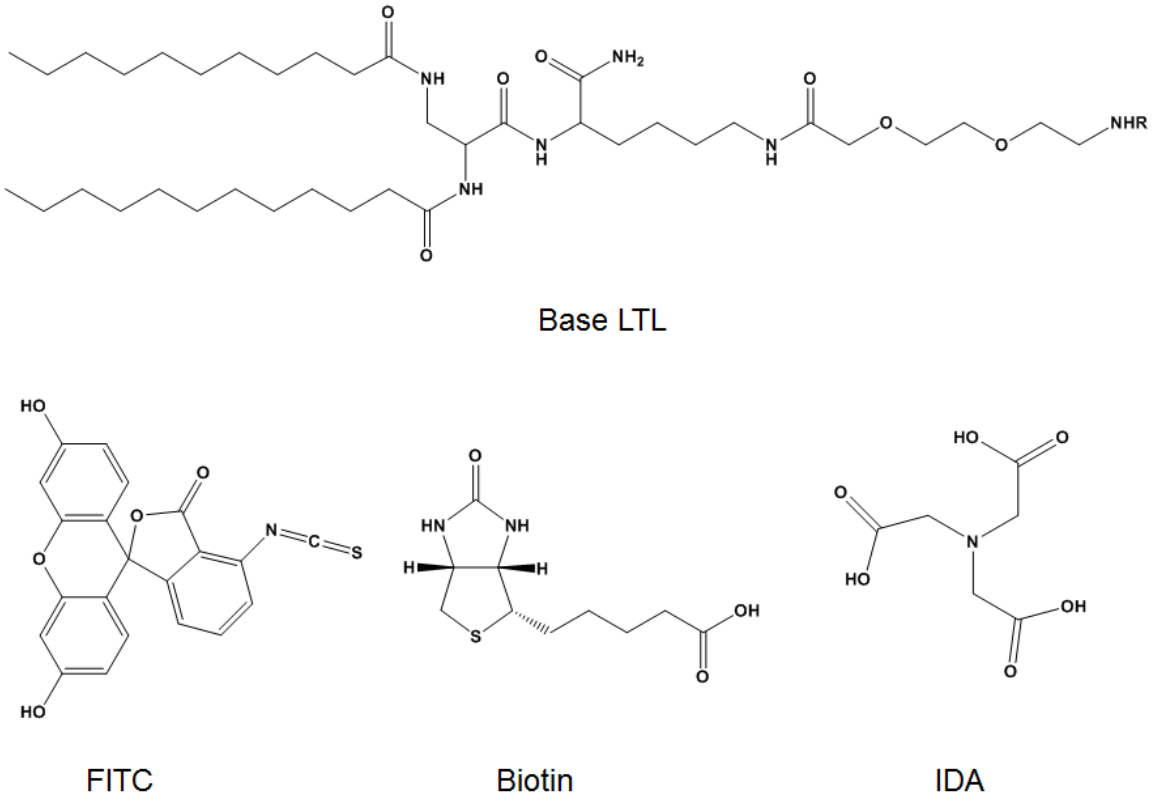

Figure 3.1 Chemical structures of the base LTL, the FITC head group, the biotin head group, and the IDA head group employed in these studies.

While the LTL strategy continues to be exploited on C-CP fibers, it is reasonable to believe that the approach may have far-reaching application. The goal of the present work is to demonstrate the general utility of the LTL methodology through the modification of standard, commercially available PS-DVB bead material. These materials enjoy widespread use in various chromatographic and solid phase extraction platforms, though the breadth of the applications could be extended through the use of more facile surface modification procedures. We present here preliminary evaluation of the LTL surface modification operating space as well as quantitative assessment of the

surface ligand densities. The efficacy of the approach is demonstrated through the modification of the PS-DVB surface with biotinylated LTLs, and the selective capture of Texas Red-labeled streptavidin (SAv-TR) in the presence of other proteins (green fluorescent protein). While there is further optimization to be done, the preliminary results are quite promising and suggest the modification of other hydrophobic chromatography supports using LTLs.

EXPERIMENTAL

Materials

Fluorescein isocyanate (FITC)- and biotin-modified lipid tethered ligands were synthesized according to the procedure published by Marcus et al. [103] using commercially available sources and a standard solid phase synthesis methodology. The LTL was washed with ether to remove impurities after cleavage from the Rink amide MBHA resin, with stock solutions stored in a freezer at a 1 mg mL^{-1} concentration in dimethyl sulfoxide (DMSO). StatoShpere PL-PS/DVB resin (100-200 mesh), 1% cross-linked with divinylbenzene, was purchased from Sigma-Aldrich (Milwaukee, WI). Ethanol (EtOH), methanol (MeOH), and acetonitrile (ACN) were obtained from Fisher Scientific (Pittsburg, PA). Deionized water (18.2MΩ, DI-H_2O) was generated in-house. Bovine serum albumin (BSA) was purchased from Sigma-Aldrich. Phosphate buffered saline (PBS buffer) was prepared with 140 mM NaCl, 10mM Na_2HPO_4, 1.8 mM KH_2PO_4, and 2.7 mM KCl at a pH of 7.3 (Sigma-Aldrich). Texas Red labeled streptavidin (SAv-TR) was purchased from SouthernBiotech (Birmingham,

AL). Enhanced green fluorescent protein (EGFP) (derived from p3051 retrovirus vector and amplified by PCR) was provided by Dr. G. Chumanov of the Chemistry Department of Clemson University (Clemson, SC). Tween-20 was purchased from Rockland Immunochemicals Inc. (Gilbertsville,PA)

Equipment

Fluorescence images were taken using an Olympus IX71, 2x/0.08 UPlanFI (infinity corrected) objective (Olympus, Center Valley, PA). Excitation was affected using a xenon arc lamp. The excitation/emission wavelengths were as follows: 494 nm/525 nm for FITC-LTL and 575 nm/624 nm for SAv-TR. UV-VIS measurements were made using the flow through microcuvette of a Dionex Ultimate 300 HPLC system (LPG-3400SD pump, WPS-3000TSl autosampler, VWD-3400 RS UV-Vis absorbance detector, Thermo-Fisher Scientific, Sunnyvale, CA). Measurements were always taken at a flow rate of 1 mL min^{-1} and an injection volume of 20 μL. FITC-LTL concentrations were determined at 495 nm and SAv-TR at 590 nm. The solvent composition in the HPLC flow was 40:60 ethanol:water by volume (*sic* 40% EtOH) unless otherwise stated. Tumbling of the solutions was accomplished with a modified rotary evaporator, where the condenser was replaced with a wooden block. Sample vials were affixed to the block by rubber bands and agitated as the unit rotated.

Evaluation of LTL adsorption under different solvent conditions

The adsorption of the LTLs to the PS-DVB was evaluated using different solvents, ACN, MeOH and EtOH, and volume fractions ranging from 30-70% of

the organic modifier in DI-H_2O. These solutions were used as diluents to make 10 µg mL^{-1} FITC-LTL working solutions from the 1 mg mL^{-1} initial stock. The FITC-LTL solutions were sonicated for 1 h, shaken vigorously, and then sonicated for another hour to ensure solvation. Four solid phase extraction cartridges were loaded with 20 mg of PS-DVB resin. Each cartridge received 1 mL of a FITC-LTL test solution; one solvent composition per cartridge. The cartridges were capped and tumbled for 30 min to load the resin with the FITC-LTL. The cartridge containing the FITC-LTL-PS-DVB beads was drained of excess solution. The FITC-LTL resin was then washed in triplicate with 1 mL portions of DI-H_2O. The resulting resin was left to dry under house vacuum for 24 h, after which the resin was plated onto a slide for fluorescence imaging.

Evaluation of LTL adsorption through quantification of primary solution depletion

Samples of FITC-LTL stock solution were exposed to PS-DVB to determine the adsorption behavior, with the amount adsorbed determined by the depletion of the LTL from the stock solution. 25 µl of the 1mg mL^{-1} FITC-LTL stock solution was diluted in a 25 mL volumetric flask with 40:60 EtOH:H_2O. The 10 µg mL^{-1} FITC-LTL solution was sonicated for 1 h, shaken vigorously, and sonicated for another hour. In the determination of the equilibrium loading capacity, four sets of three autosampler vials were filled with varying masses of PS-DVB resin. The four weights used were approximately 10, 25, 40, 50, 100, 150 mg (±2.5 mg) of resin. The pipettes used for the solution transfer were first

conditioned with 1 mL of the 10 µg mL^{-1} LTL solution to passivate the surfaces. Each resin sample received 1 mL of the prepared 10 µg mL^{-1} FITC-LTL solution. The vials were then tumbled for 30 min. After the allotted time, the vials were left to settle, then a 750 µl sample of the resulting LTL-depleted solution was extracted with a glass pipette and transferred to a new autosampler vial. The final concentration of the FITC-LTL was determined via UV-VIS absorbance, with the difference between the original and determined values assumed to represent that amount adsorbed to the beads.

Adsorption of FITC-LTL was also evaluated to determine the optimum exposure time. 50 µl of the 1 mg mL^{-1} FITC-LTL stock solution was diluted in 50 mL volumetric flask with 40% EtOH. The 10 µg mL^{-1} FITC-LTL solution was sonicated for one hour, shaken vigorously, and sonicated for another hour. 30 autosampler vials were filled with approximately 50 mg each of PS-DVB resin. The pipette used for the following solution transfer was conditioned with 1 mL of FITC-LTL. Each of the 30 samples was loaded with 1 mL of 10 µg mL^{-1} FITC-LTL. The vials were placed on the modified rotovap and tumbled, with three removed at 1, 2, 5, 10, 30, 60, 180, 360, and 720 min incubation times respectively. After a set of vials was removed, and the resin allowed to settle, 0.75 mL of depleted LTL solution was transferred to new autosampler vials. At the end of the 24 hours the supernatants were analyzed by UV-VIS to determine the extent of FITC-LTL depletion.

Streptavidin-Texas Red capture by biotin-LTL-modified PS-DVB

Depletion of the SAv-TR from a primary solution was used to quantify the loading of affinity ligands to the polymer beads. 25 µl of the 1 mg mL^{-1} biotin-LTL stock solution was diluted in a 25 mL volumetric flask with 40% EtOH. The 10 µg mL^{-1} biotin-LTL solution was sonicated for one hour, shaken vigorously, and sonicated for another hour. 30 autosampler vials were filled with approximately 50 mg of PS-DVB resin each. The pipette used for the following solution transfer was conditioned with 1 mL of biotin-LTL. Fifteen of the vials were filled only with 1 mL of 40% EtOH for use as a negative control (no ligand), while the other 15 vials were filled with 1 mL of the 10 µg mL^{-1} biotin-LTL solution. The vials were tumbled for 1 h and drained of excess solution and washed with DI-H_2O in triplicate. The native and functionalized resins were dried under house vacuum for 24 hours and then reweighed prior to transfer to glass autosampler vials. A 60 µg mL^{-1} stock solution of SAv-TR was made in buffer, and dilutions (1, 5, 10, 20, and 60 µg mL^{-1}) prepared. 1 mL of each SAv-TR concentration was added to six separate vials, three biotin-LTL functionalized PS-DVB samples and three PS-DVB controls. The vials were tumbled for five minutes. After tumbling, a 0.75 mL sample of the LTL-depleted solution was extracted for analysis and put into new vials using a glass pipette. The supernatants (20 µL aliquots) were analyzed by UV-Vis to determine the extent of SAv-TR depletion with the HPLC carrier solution being PBS buffer.

Samples of 50mg PS-DVB resin were prepared with biotin-LTL as described above. The samples were then divided into seven groups and washed

with differing pH solutions at 1,3,5,7,9,11, and 13. A wash consisted of a 1ml wash volume, vortex mixing for 1 minute, followed by 5 minutes static exposure to let the resin settle out. Washes were done in triplicate. These samples were then washed again in triplicate with PBS buffer to adjust the pH back to neutral before SAv-TR exposure. A loading solution of 10ppm SAv-TR was used and depletion of that solution was monitored by UV-Vis.

Confirmation of Texas Red-labeled streptavidin immobilization on PS-DVB resin by fluorescence microscopy

The PS-DVB resin was functionalized with the biotin-LTL as described in the previous section. One vial contained a PS-DVB negative control, and the other was a sample of the biotin-LTL-modified PS-DVB resin. Both vials were exposed to a solution containing 5 μg mL^{-1} each of SAv-TR, and EGFP in PBS buffer. The vials were tumbled on the modified rotovap for 5 min. The resin samples were washed with 1 mL of DI-H_2O, in triplicate. The samples were then suspended in water, and a small sample of resin removed with a pasture pipette and spotted onto a glass slide. Fluorescence images were taken separately (different excitation/emission wavelengths) to evaluate the presence of SAv-TR and EGFP on the PS-DVB resin. The samples were then dried for 24 hours under house vacuum and reimaged to ensure that the imaging results were not skewed by solvent effects.

Methods to minimize non-specific binding

The addition of Tween-20 to test solutions and the use of a BSA surface block are common methods to minimize non-specific binding to chromatographic supports. Both approaches were evaluated here to assess their utility. 10 µl of the 1 mg mL^{-1} biotin-LTL stock solution was diluted in 10 mL volumetric flask with 40% EtOH. The solution was prepared in the same fashion as the previous solutions. Four 20 mg samples of PS-DVB resin were weighed and placed into auto sampler vials. Three of the vials were treated with 1 mL of the 10 µg mL^{-1} biotin-LTL solution, while one simply wet with 40% EtOH as a negative control. The vials were all tumbled for 1 h. The resin was then washed as described in the previous sections. One of the vials was then loaded with 1 mL of 20 µg mL^{-1} bovine serum albumin (BSA) in water, and tumbled for an additional 10 min and drained. The four vials were then loaded with 1 mL of 5 µg mL^{-1} SAv-TR solution. One of the load aliquots contained 0.1% Tween-20. These were then tumbled for 5 min and cleaned. Each sample was plated onto a glass slide and dried in a vacuum desiccator. Once the resin was dried, fluorescence images were taken to assess SAv-TR capture.

In the second set of experiments interrogated the potential elution of the LTL from the PS-DVB beads. Two 20 mg samples of resin were weighed and added to auto sampler vials. The vials were loaded with 1 mL of 10 µg mL^{-1} biotin-LTL. The resin was loaded and cleaned as described above. Each sample was then exposed to 5 µg mL^{-1} SAv-TR in water, and tumbled for 5 min and washed. An additional wash was added where one sample was exposed to

1 mL of 0.1% aqueous Tween-20, while the other was exposed to only 1 mL of DI-H_2O. Each vial was tumbled for 5 min, the resin plated onto the slides, and dried prior to imaging for the presence of SAv-TR on the bead surface.

IDA-LTL and the extraction of methylene blue

Three 50mg samples of resin were loaded with 10ppm IDA-LTL using the procedure outlined above, while three 50mg samples were kept as controls. The samples were washed with distilled water in triplicate. The IDA-LTL functionalized resin was then exposed to 1 ml of 2.8ppm methylene blue and shaken by hand. The resin was allowed to settle out of solution, and the resulting solution phase was extracted for analysis. The resin was then washed in triplicate with deionized water and the wash solutions were extracted for analysis. After three washes no methylene blue was seen in the control, and minimal leaching from the resin was observed. The remaining methylene blue was then eluted with 1ml pH 1 HCl solution, the solution phase was extracted for analysis. The solutions were quantified by UV-Vis.

RESULTS AND DISCUSSION

Previous efforts implementing the lipid-tethered ligands on polypropylene C-CP fiber surfaces yielded a very simple, efficient application methodology. Fibers co-linearly packed into column structures are modified simply by passing the LTLs in 50:50 EtOH:H_2O solvent under flow conditions (solvent linear velocity of 10-50 mm s^{-1}), with the surfaces densely populated on time scales of just a few seconds [48,102,103]. This process probably represents the best-case scenario

for several reasons. First, the lipid tails have an extremely high affinity for the polypropylene matrix [104]. Second, the mass transport of solutes to the surface is very efficient due to the high sheer conditions [101]. Finally, the virtual lack of surface porosity means that the overall loading rate is not limited by the need for ligands to diffuse through pores to reach all support surfaces [105]. Extension of the methodology to porous, PS-DVB media brings a different set of chemical and physical parameters to the basic adsorption processes, which are addressed here. Key variables include the identity and percentage of organic modifier in the loading solution, the optimization of the resin to loading solution ratio, and the amount of time the resin is exposed to the LTL. Optimized conditions were chosen based on these results.

Effect of solution composition for FITC-LTL loading onto PS-DVB

There are certainly competitive processes in effect in the immobilization of the lipid onto the hydrophobic PS-DVB surface. One would expect an equilibrium situation based on the relative solubility of the LTL in the mixed-solvent phase and the affinity of the hydrophobic lipid tail towards the support material. PS-DVB resin was exposed to 10 µg mL^{-1} FICT-LTL at differing concentrations of EtOH, and agitated for 30 minutes, with the extent of immobilization assessed by fluorescence microscopy. **Figure 3.2** depicts the dramatic effect that solvent composition has on the FITC-LTL adsorption for compositions of 40 to 70% EtOH. The fluorescence images from the 50, 60 samples are fairly similar when

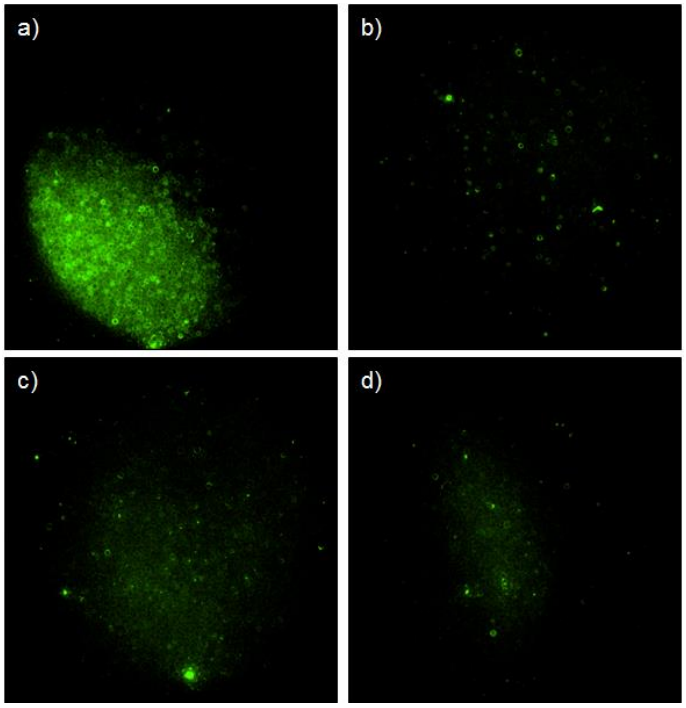

Figure 3.2 Fluorescence images of FITC-LTL adsorbed on PS-DVB resin illustrating the impact of solvent composition on LTL adsorption. Lipids were loaded at aqueous ethanol concentrations of a) 40%, b) 50%, c) 60%, and d) 70%. Images were taken under the same excitation/ measurement conditions.

contrasted against the 40% EtOH case, which reflects vastly superior LTL adsorption to the PS-DVB beads. It should be noted that 20 and 30% ethanolic solutions were prepared, but at a concentration of 10 µg mL^{-1} the FITC-LTL precipitated out of solution. The images (taken after solvent removal to alleviate spectroscopic solvent effects) clearly suggest that as the solution becomes more organic/less polar the adsorption of the LTL to PS-DVB is suppressed. Under the optimal loading conditions, LTL solubility is balanced with the adsorption affinity to the PS-DVB surface. Complementary experiments were performed with the other two most commonly used HPLC solvents, ACN and MeOH as the organic modifiers. The general solubility of the LTL in these solvents was similar to that of EtOH, but the surface adsorption was poor at 30% for both ACN and MeOH, and could not be detected by the fluorescence microscope for the organic

content of greater than 40% for either of these solvents. Therefore, 10 μg mL^{-1} solutions of LTL in 40% EtOH were used as the deposition solution for all subsequent LTL surface modifications.

Quantitative characterization of FITC-LTL adsorption onto PS-DVB media

The adsorption of the FITC-LTL was characterized in relation to both exposure time and the mass of the resin exposed to the load solution. Because of the hydrophobic nature of the lipid tails, lipid contact with polymer-based materials must be limited. For example, it was found that statistically significant, non-reproducible amounts of material will adsorb to “low retention” polypropylene transfer equipment, and thus the polymer vials employed in the adsorption experiments were replaced with glass autosampler vials. It was possible to condition the other polymer-based materials to alleviate further adsorption. Pipette tips used to transfer solutions were conditioned by passing 1 mL of the 10 μg mL^{-1} FITC-LTL starting solution. This treatment yielded no further LTL adsorption in the solution transfer processes. In both sets of experiments, 1 mL aliquots of 10 μg mL^{-1} FITC-LTL in 40% EtOH were employed as the load solutions. For these quantitative measurements, the amount of LTL depleted from the load solutions was determined via UV-VIS absorbance.

The mass of bound LTL was evaluated with respect to the mass of resin (20 – 150 mg) used to deplete 1 mL of a 10 μg mL^{-1} FITC-LTL solution. It was originally expected that as the mass of the resin increased, the amount of LTL

removed from the solution would also increase proportionally. The results were evaluated with

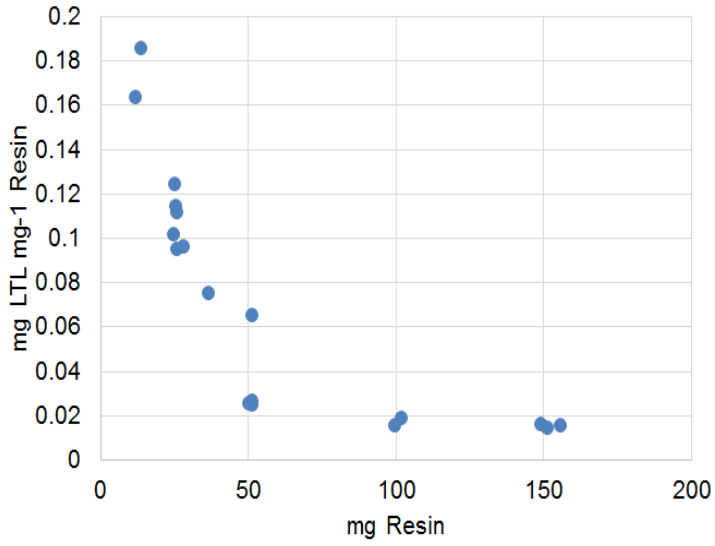

Figure 3.3 Evaluation of LTL adsorption as a function of A) mass of base resin material and B) incubation time. Test solutions in both cases were 1 mL of 10 □g mL-1 FITC-LTL in 40% ethanol solvent, with amount bound assessed by LTL depletion from the starting solution. 50 mg of PS-DVB resin employed in temporal studies.

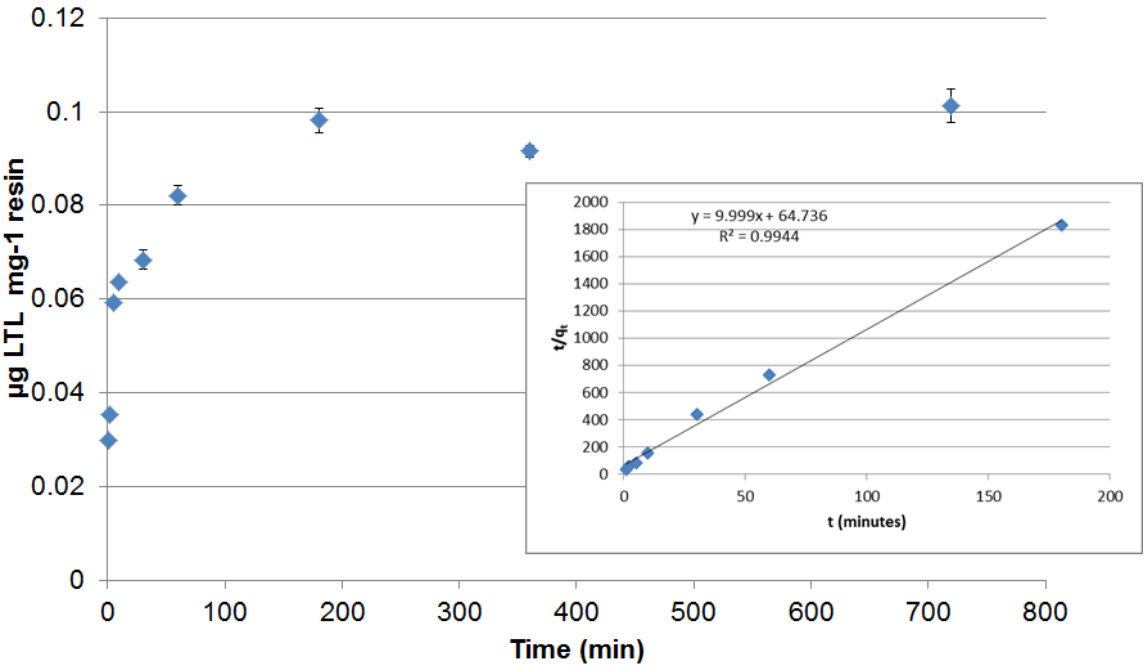

respect to mass (mg^{-1}) of PS-DVB resin. As seen in **Figure 3.3A**, the amount of adsorbed LTL per mass of resin decreased dramatically as a function of exposed

bead mass. In fact, the amount of FITC-LTL depleted from solution did not change significantly in relation to the amount of PS-DVB resin it was exposed, with the resulting solution in all cases depleted from 10 μg mL^{-1} to ~7 to 8.5 μg mL^{-1} when incubated for 30 min. The data suggests that the driving force of LTL adsorption is the equilibrium between two concentrations of LTL, the near-saturated solution at 10 μg mL^{-1} and an equilibrium solution concentration of ~8 μg mL^{-1}. Once the solution is depleted to near 8 μg mL^{-1}, further LTL adsorption is ill-favored, regardless of the amount of resin substrate. Based on these measurements 50 mg of resin was chosen to be a suitable amount of resin to be used for depletion of 1 mL of the FITC-LTL test solution.

Very different from the case of the (virtually) non-porous C-CP fiber phase where transport to the near flat surface region controls the adsorption kinetics [105], there is a further diffusive component to the LTL access to the PS-DVB pore surfaces and further morphology. The temporal characteristics of the LTL adsorption was evaluated using ~50 mg of PS-DVB resin for all tests. **Figure 3.3B** presents a graph of the FITC-LTL loading on the polymer resin beads, normalized to the mass of the resin, for triplicate experiments as a function of incubation time. As can be seen, the amount of adsorbed lipid increases rapidly over the first hour or so. The data show that beyond 3 h the additional adsorption gained is insignificant in comparison to the increased exposure time. There are many approaches to assessing these sorts of adsorption processes [106]. A straight forward fit of the adsorption data to an equation of the form

$$t/q_t = (1/V_o) + (1/q_e)t \qquad [1]$$

where q_t is the mass of LTL adsorbed per mass unit of beads at a given incubation time, and V_o and q_e represent the y-intercept and the inverse of the slope of the plot insert of **Figure 3.3B**, allows calculation of the second-order adsorption rate constant k.

$$k = (V_o/q_e^2)^{1/2} \qquad [2]$$

Based on the data fit to equation [2], the rate constant for the LTL adsorption is 1.54 g resin (mg LTL*min)$^{-1}$. This value is very different from the C-CP dynamic loading of first generation LTLs, which saturates to values of ~1.6 mg LTL per gram of fiber under flow conditions on time scales of a few seconds [48]. It is noted that the load rate on C-CP fibers is ~100X that of the PS-DVB system. It is interesting to note that the computed equilibrium capacity (q_e) based on the fit of the data to Eq. 1, matches the experimental equilibrium binding capacity of 0.1 μg LTL/mg bead depicted in **Figure 3.3B**. The goodness of fit of Eq. 1 and the self-consistency with the experimental q_e value support the case where pseudo-second-order kinetics adsorption is taking place. The pseudo-second-order rate kinetics is reasonable as the rate will depend on both the concentration of LTL in the loading solution and the availability of surface binding sites. PS-DVB micro particles are porous, but the extent of the porosity is dependent on the solvent conditions which swells the resin, the more hydrophobic the greater the swelling. The PS-DVB is exposed to the most hydrophobic solvent conditions during LTL

loading; for the functional use of the LTL-Resin in this study. It is reasonable to expect that the porosity of the PS-DVB resin is highest in the loading conditions than at any other point, caused by solvent swelling. Swelling of the resin will cause more binding sites to become available for LTL adsorption. Following the wash cycles the resin would shrink, trapping LTL in sections of the porous structure. Full permeation of the LTL into the porous structure is unlikely as the degree of swelling is severely limited by the hydrophobicity of the solvent. This effect does not entirely explain the 1.5% utilization and most likely has less of an influence than the steric concerns of adjacent SAv-TR molecules.

Selective capture of streptavidin by biotin-LTL functionalized resin

A biotin-LTL bound to polypropylene C-CP fibers has previously been used to extract SAv-TR from cell lysate with very high selectivity [102]. PS-DVB resin was modified with the biotin-LTL using the parameters derived above (10 $\mu g\ mL^{-1}$ ligand in 40% EtOH on 50 mg resin for 1 h incubation), with unmodified PS-DVB beads used as a control to evaluate non-specific binding to the polymer surface. The samples were exposed to a solution containing a mixture of 5 $\mu g\ mL^{-1}$ SAv-TR and 5 $\mu g\ mL^{-1}$ enhanced green fluorescent protein (EGFP) in PBS buffer. EGFP is used here to reflect the non-specific protein binding to both resin surfaces. The images in **Figure 3.4A** and **C** clearly reflect the fact that both proteins have an affinity for the native PS-DVB matrices, as would be expected. Upon functionalization with the biotin-LTL, there is a very large increase in the amount of SAv-TR on the surface as reflected in the increased fluorescence

intensities of **Figure 3.4B**, plotted on the same scale as the control of **Figure 3.4A**. At the same time, there is an appreciable decrease in the fluorescence signal observed from the EGFP in the biotin-LTL modified case (**Figure 3.4D**)

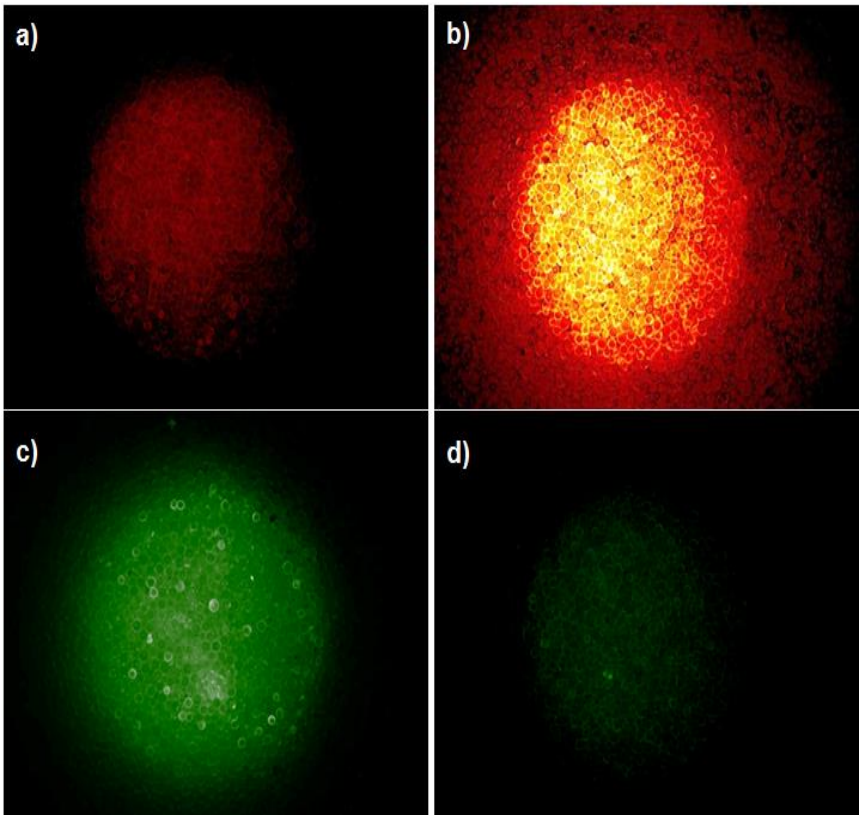

Figure 3.4 Fluorescence images of PS-DVB resin beads following exposure to 5 □g mL^{-1} SAv-TR and 5 □g mL^{-1} EGFP. Images **A**) and **C**) reflect unmodified PS-DVB and **B**) and **D**) those of biotin-LTL modified PS-DVB beads. SAv-TR images **A**) and **B**); EGFP images **C**) and **D**). Florescent intensity scaling is consistent for each probe ligand type.

versus the unmodified material (**Figure 3.4C**). This inhibition of non-specific EGFP binding is likely a combination of a change in the surface hydrophobicity upon modification with the LTL and a steric exclusion of the EGFP by the bound SAv-TR. These samples were dried and reimaged to ensure that solvent effects were not responsible for the change in fluorescence.

Efficiency of streptavidin capture by biotin-LTL functionalized PS-DVB

The biotin-streptavidin interaction is the strongest known non-covalent interaction with a dissociation constant $K_d = 10^{-14}$ M [107]. As such, the amount of SAv-TR captured by the surface-bound biotin-LTL is limited by the number of LTLs on the surface, the density of the ligands and the physical accessibility of the protein to those ligands. Ligands spacing smaller than the physical size of SAv have diminishing utility. Likewise, ligands in pores that are not accessible by the protein are also wasted. Under the assumption that the densities of adsorbed biotin-LTL and FITC-LTL are comparable, the total amount of ligand on 50 mg of the bead material should be ~4.4×10^{-9} moles. Therefore, based on the best-case (and practically unlikely) scenario of a 1:1 biotin:SAv capture ratio, an equal number of moles could be captured on the bead material, equivalent to 0.24 mg of SAv (MW = 55,000 Da) for 50 mg of the bead material.

The extent of SAv-TR capture was evaluated by depletion of a primary SAv-TR solution. As in the case above, ~50mg of resin was modified with 1 mL of 10 μg mL^{-1} biotin-LTL in 40% EtOH. Triplicate measurements of SAv-TR depletion from 1 mL protein test solutions were performed over the protein concentration range of 5 - 60 μg $mL^{-1.}$ Based on the premise of the ideal, 100% capture efficiency, the amount of immobilized ligand should completely deplete each of the solutions; this was not the case. In fact, the amount of immobilized protein was averaged 3.4 μg, varying little with the solution concentration. With the current method of detection no less than 5 μg mL^{-1} SAv-TR loading solution can be used due to an LOQ of 1.33 μg mL^{-1}. The consistency in SAv-TR

extraction indicates that all of the available Biotin-LTLs are occupied even at low concentration. The SAv-TR protein-dye conjugate is very large, and has four biotin binding site. Additional binding sites allows for the potential of at least two LTLs binding per SAv-TR. Steric interactions will play an important role, as the addition on a single SAv-TR will block access to many adjacent LTLs on the surface. Surface morphology is an additional consideration as LTLs will gain more access to valleys and into the porous material in comparison to the SAv-TR. A single SA-vTR could block access to a valley with functionalized with LTL. Thus the capture efficiency, per molar unit of immobilized ligand, was ~1.5%. This is not an unreasonable value at this stage of method development. Greater utilization might be realized by reducing the ligand surface density, but limitations inflicted by pore access cannot be remedied. Of course, this approach may lead to greater non-specific binding to the PS-DVB.

It is critical that the adsorbed LTL can remain stable in typical elution conditions used in affinity chromatography. The most common elution condition for affinity chromatography is a simply pH change. Other common elution conditions are competitive binding, ionic strength, and chaotropic elution. These are specific to the affinity system being examined, but should have no impact of LTL stability as these conditions are not highly reactive or increase the hydrophobicity of the solvent system. LTL stability as a function of pH is critical, as most affinity chromatography occurs with a simple change in pH. The stability of the biotin-LTL adsorbed to PS-DVB is displayed in **Figure 3.5**. **Figure 3.5**

show the percentage of streptavidin captured from 1ml 10ppm aliquot using approximately 50mg PS-DVB resin functionalized with biotin-LTL as described above. It is clear that even under more extreme pH conditions the stability of the

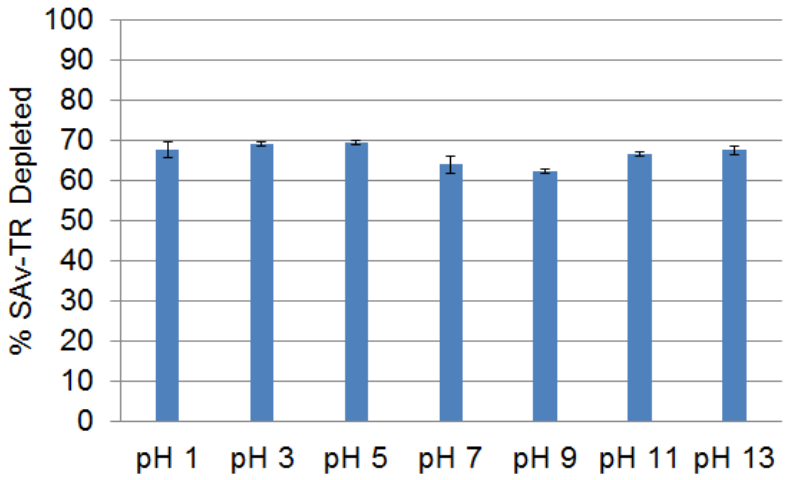

Figure 3.5 Depletion of a 10ppm SAv-TR solution by biotin-LTL post exposure to different pH conditions. Variance is a result of deferring amounts of resin used, and sample loss due to extensive washing.

LTL was not compromised as ~65% of the SAv-TR was captured in all cases. It is important to note that the pH was adjusted back to 7.3 with three replicate washes with PBS buffer prior to SAv-TR capture.

Evaluation of two common methods to minimize non-specific binding

The occurrence of non-specific binding events not only lessens the derived purity in a preparative separation, but also leads to lower overall yields for the target protein. Two the most common means of inhibiting non-specific binding are the addition of detergents to the feedstock or coating the support with bovine serum albumin (BSA) following the immobilization of the capture ligands. This so-called *BSA-block* back-fills the support surface, prohibiting egress and subsequent adsorption of proteins to the support surface. Tween-20 is commonly used at concentrations of 0.01-1% to inhibit the non-specific binding of

proteins to hydrophobic surfaces. Tween-20 is a detergent, and all detergents are amphipathic, and as a result the hydrophobic regions of the detergent will align with the hydrophobic regions of a protein, or LTL. Tween-20 and Triton X-100 are both commonly used because they are non-ionic detergents. Ionic detergents are biologically harsher as they tend to cause greater structural changes to proteins. They are also more sensitive to changes in ionic strength and pH, and may interfere with downstream methods that require charged species. In our past work, inclusion of 0.1% Tween-20 in cell lysate eliminated non-specific binding to bare polypropylene C-CP fiber surfaces [102,103]. By the same token, the adsorption of the LTL to the polypropylene surfaces was not thoroughly disrupted by exposure to the detergent. The effects of Tween-20 on the biotin-LTL functionalized PS-DVB resin were evaluated by fluorescence microscopy as illustrated in **Figure 6**. The control case of SAv-TR adsorption to the biotin-LTL on PS-DVB is shown in **Figure 6A**. Exposure of that system to a 0.1% tween-20 solution drastically reduced the apparent amount of SAv-TR on the surface based on the fluorescence image of **Figure 6B**. One of two things is likely happening, either the Tween-20 causes the LTL to desorb from the surface or in some way was decoupling the biotin-SAv interaction (admittedly an unlikely event). The potential perturbation of the LTL-surface coupling was assessed by adding 0.1 % Tween to the SAv-TR test solution which was then exposed to the LTL-modified beads. In this case, indeed very little of the SAv-TR was selectively adsorbed as seen in the images of **Figure 6C** and **D**. To reiterate,

this situation caused no significant change in the selective capture of SAv on the LTL-modified C-CP fibers. As such, it is not the biotin-SAv interaction that is

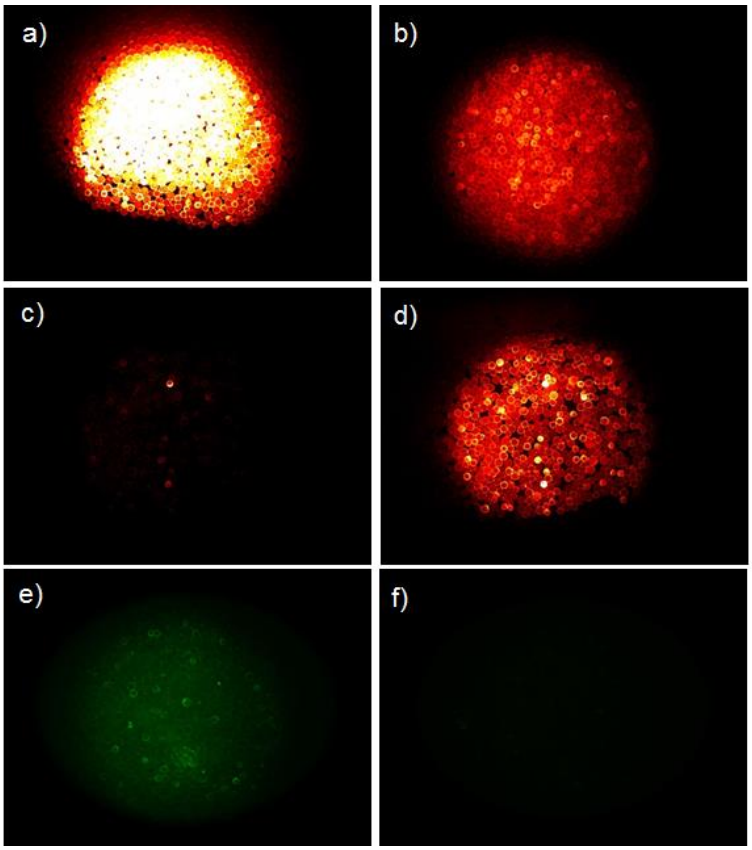

Figure 3.6 Fluorescence images illustrating the effects of exposure to 0.1% Tween solutions. a) Selective SAv-TR capture on biotin-LTL modified PS-DVB. b) Exposure of captured SAv-TR to 0.1% Tween solution with intensity scale expansion of ~6x. c) Capture of SAv-TR in the presence of 0.1% Tween in the primary solution. d) Same as c), but with intensity scale expansion of ~6x. e) FITC-LTL modified PS-DVB. f) FITC-LTL modification of PS-DVB in the presence of 0.1% Tween. Florescent intensity scaling consistent for each probe ligand type, unless stated otherwise.

perturbed, but that the LTL is no longer present for surface capture; i.e., the LTL is liberated in the presence of the detergent. This conclusion is further supported by comparing the fluorescence image of FITC-LTL-modified PS-DVB beads (**Figure 6E**) and that following 5 min exposure of that surface to the 0.1% Tween solution (**Figure 6F**). Clearly, the fluorescence is dramatically reduced. Indeed, high levels of FITC fluorescence where obtained in the Tween wash solution. Thus, it is clear that the interactions between the aliphatic lipid tails with the aromatic-natured PS-DVB are far less robust than those with the

polypropylene C-CP fiber matrix. Ultimately, the use of tween to suppress non-specific binding is counterproductive.

BSA blocks are used to occupy hydrophobic sites on supports (absent of ligands), sterically blocking access of the proteins in solution to the surface. Even as BSA does not have an affinity to biotin, there could be some

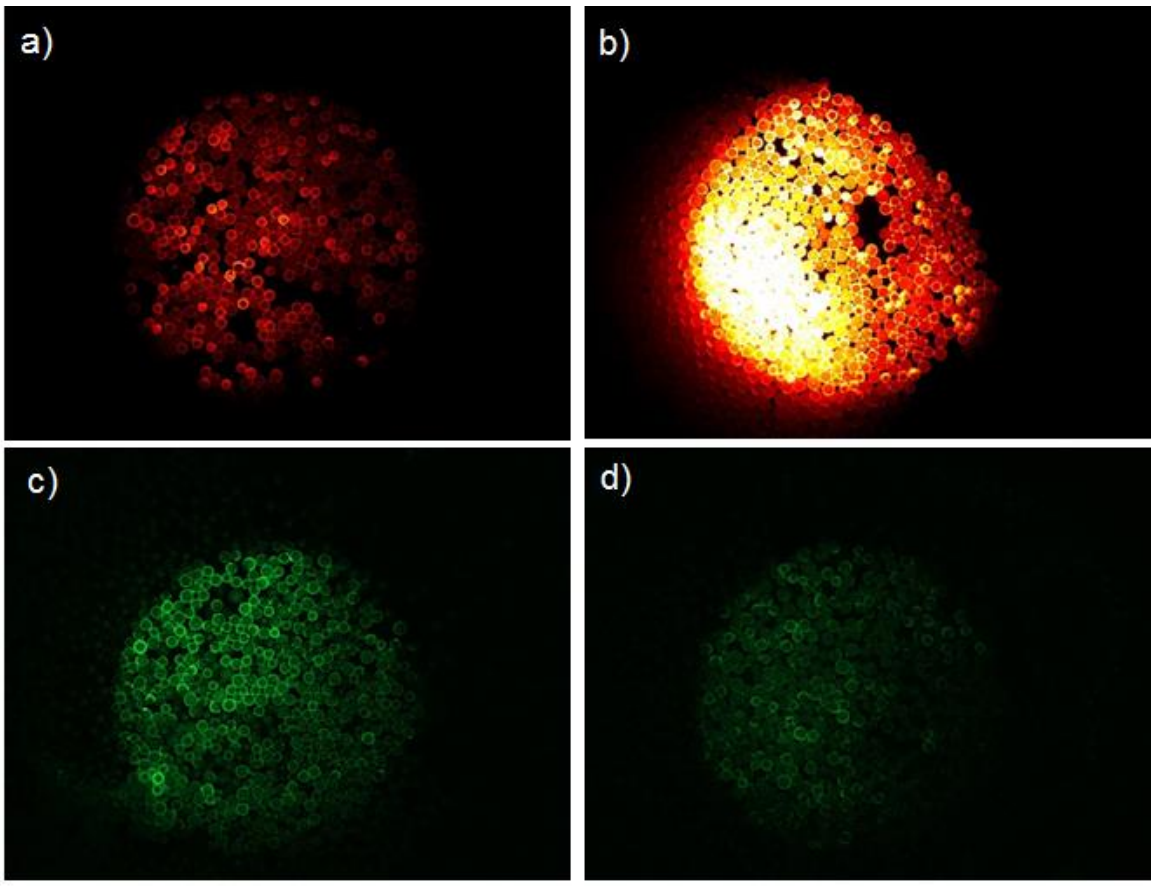

Figure 3.7 Fluorescence images illustrating the effects of BSA surface blocking following initial adsorption of biotin-LTL on PS-DVB. Images a) and c) reflect unmodified PS-DVB and b) and d) those of biotin-LTL modified PS-DVB beads. SAv-TR images a) and b); EGFP images c) and d). Florescence intensity scaling consistent for each protein type.

BSA blocking access of the SAv-TR to the biotin-LTL surface ligands due to its shear size relative to the LTL. Considering the native PS-DVB surface being the extreme case for non-specific protein binding, the images of **Figure 3.7A** and **C** illustrate the full extent of non-specific adsorption of SAv-TR and EGFP. Clearly, non-specific binding is taking place. Exposure of the biotin-LTL-modified PS-DVB to the BSA blocking solution should provide for a barrier to non-specific binding, hopefully without impeding SAv-TR capture. The SAv-TR and EGFP test solutions were exposed to biotin-LTL beads following the BSA treatment. As seen in the fluorescence image of **Figure 3.7B**, there appears to be no impediment to SAv capture in the presence of the BSA block, as this image and that of **Figure 3.7A** are very comparable. To the contrary, exposure of the EGFP solution to that surface resulted in a reduced amount of non-specific binding (**Figure 3.7D**). Although the EGFP images **Figure 3.4** and **Figure 3.7** are not directly comparable due to different scales, the raw data fluorescence intensity can be examined. The average fluorescent intensity for **Figure 3.4D** is 780 and that of **Figure 3.7A** is 515. Thus, it appears that a simple BSA blocking step, as is common throughout the bioseparations arena, is a simple and practical means of alleviating non-specific binding in the case of LTL-modified PS-DVB media. To this end, as suggested in the inhibition of EGFP binding in the presence of the biotin-LTL, a mixed surface of biotin-LTL and a simple hydroxyl-LTL may achieve better utilization without the penalty of non-specific binding.

Application of LTL modality for utilizing iminodiacetic acid-LTL

To this point two systems have been used to examine how the LTL adsorbs to PS-DVB, and how is can be used to extract biomolecules solution. The FITC-LTL allowed quantitation of LTL loading kinetics and the optimization of loading conditions. The interaction of SAv and biotin is a powerful model system to illustrate how the LTL modality can be used to extract select proteins from solution. It also allowed for the quantification of ligand utilization. Unfortunately, the incredibly strong interaction that makes this such a model system requires

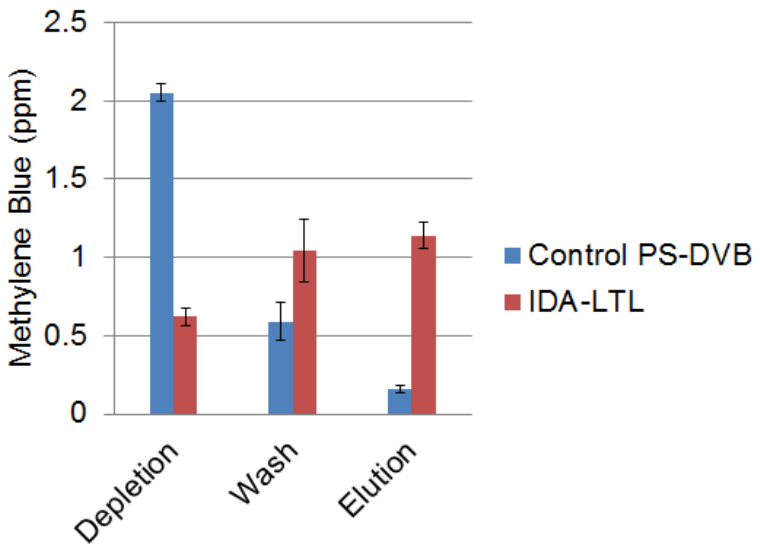

Figure 3.8 Extraction of 1ml of 2.8 ppm methylene blue from solution using IDA-LTL. Samples are evaluated post depletion, during each wash phase, and elution. Elution wash achieved with 1ml of pH 1 HCl. All of the wash solutions analyzed were added together to illustrate total sample lost to washing.

exceeding harsh elution conditions. An LTL was synthesized with an iminodiacetic acid (IDA) head group. The two carboxylic acid function groups are deprotonated at neutral pH, yielding two anions that can be used as a model for more complex affinity systems. The IDA-LTL can be used as a model system to present a similar mechanism commonly used in affinity chromatography. Biomolecular affinity of a ligand to a binding site can normally be modulated by a

shift in pH. This causes a change in the degree of ionization in either (or both) the ligand or the protein. This method is commonly used to reduce the coulombic forces associated with a ligand-protein affinity complex. In this study the cationic dye methylene blue was use to probe the system. It can be seen in **Figure 3.8** that the IDA-LTL functioned PS-DVB resin depleted the methylene blue in a neutral solution. IDA presents two carboxylate anions at neutral pH which will interact with cationic species, extracting methylene blue from solution. The resin was then washed in triplicate and the remaining methylene blue was eluted from the functionalized resin using a hydrochloric acid solution at pH 1. When the pH was decreased to 1 the acid protonated the carboxylic acids of IDA eliminating the strong coulombic attraction between opposite charges, releasing the remaining methylene blue into solution.

CONCLUSIONS

The lipid tethered ligand surface modification modality has been applied to polystyrene-divinylbenzene (PS-DVB) resin media. LTL adsorption was assessed with FITC- and biotin-functionalized variants. The system was evaluated in relation to loading solvent composition, the mass of base resin, and exposure time. Proof of concept work was accomplished by extracting SAv-TR selectively from solution. The selective SAv-TR capture illustrates the potential for general use of the LTL strategy in affinity chromatography on PS-DVB supports. At this early stage, the ligand utilization is a reasonable value of ~1.4%, though more direct studies controlling ligand density are may improve

efficiency. Stability of the LTL adsorption was shown to be high, even at extreme pH. The capture and elution of methylene blue using IDA-LTL displays how the LTL modality would function with pH elution common to affinity separations. The issue of non-specific binding was addressed and the efficacies of two common solutions for non-specific binding were evaluated. The use of a 0.1% Tween solution resulted in the release of the LTL from the resin surface. Alternatively, it was determined that the use of a BSA block would be an easy and highly effective way to minimized non-specific binding.

The uses of the LTL coupling strategy allows for quick and simple surface modification of hydrophobic surfaces. The adverse effects of detergents in the case suggests that the aliphatic variant of the LTL does have weaker adsorption to PS-DVB than polypropylene, but this does not limit the scope of the LTL surface modification strategy. Future work will be completed evaluating LTLs as a potential immobilized metal affinity chromatography (IMAC) functionalization method. The use of simple copper chelating ligands such as iminodiacetic acid, would allow for further determination on the extent of active ligand density. IMAC is also a suitable direction for this work because common elution conditions are changes in pH, chaotropic agents, and competitive binding, none of which increase the hydrophobicity of the solvent system to a large degree. Future work evaluating the impact of lipid tail composition on LTL adsorption to different hydrophobic media will be undertaken. New lipid tail variants should include conjugated systems, aromatic rings, and extended branching. Such

modifications are easily affected in the LTL synthesis and should provide means of tailoring LTL-support interactions for different support matrices. Lipid tails that are tailor made for a specific polymer stationary phase should vastly increase the stability of the LTL on the surface. With a more stable system the use of common surfactants should no longer be a serious problem, as is the case currently with polypropylene C-CP fibers.

Chapter Four

General Conclusions and Future Work

This work has successfully characterized and evaluated the next generation PPY C-CP fiber for the application of protein chromatography. It has been determined that the PPY fiber breaks the trend of ideal packing at an interstitial fraction of ≈0.63, instead favoring an interstitial fraction of ≈0.45. The PPY fiber was able to separate the largest protein suite attempted for C-CP fiber protein separations of: ribonuclease A, cytochrome C, lysozyme, transferrin, bovine serum albumin, α-chymotrypsinogen. Possibly most important is that the PPY fibers out performed PP4, even though PP4 had superior packing uniformity, displaying linear velocity as a dominant force in C-CP fiber chromatography. This work suggests that the next generation of C-CP fibers would benefit from being a much smaller “Y” shaped fiber. The decrease in size would increase specific surface area, increase packing uniformity, and minimize the variation in the channel size. The shape allows the fiber to be packing at higher densities, achieving higher linear velocities.

The evaluation of the aliphatic LTL adsorbed onto PS-DVB resin has been completed. The results of this study indicate the LTL modified resin does have additional functionality that was not present prior to modification. Unfortunately, the surface population was smaller than would have been preferable and the stability of the LTL on the surface was troubling. The utilization of only 1.5% of total ligands on present on the resin begs the question of where on the resin

material is the LTL located. Similar studies on the non-porous C-CP fibers would allow an understanding on the impact of steric effects caused by adjacent SAv-TR. In addition, a similar study would elucidate the effects of surface morphology on further protein capture for PS-DVB resins.

A key shortcoming in the application of polypropylene C-CP fibers for reversed phase chromatography is column selectivity. In an effort to increase column efficiency a great deal of effort has been directed to the fiber morphology and surface chemistry, but advances in the solvent system have been stagnant. Understanding how pH effects retention of different proteins under reversed phase conditions would allow the chromatographer to enhance the selectivity of the column for a specific gradient. Changing the extent of ionization on a given protein would allow for more focused efforts to separate proteins with similar hydrophobic retentions. Additionally, the use of small fractions of acetone in the elution buffer has been previously used to change the selectivity of reversed phase columns for lipid separations[108]. Additional work with the solvent system could provide invaluable advances in C-CP fiber reversed phase separations.

LTL adsorption stability to a hydrophobic surface is a measure of complimentary interactions between the stationary phase and the LTL. Logically, this means that more chemically similar tails, when compared to a given support, would yield maximized adsorption stability. In the case of PS-DVB, tail modification should increase both the LTL stability and the surface population.

New LTL tails should be at as long as the current tails but incorporate extended conjugated systems are aromatic groups to provide more similar chemical interactions. The addition of a single aromatic ring to the end of the lipid tail would greatly increase the stability of the adsorbed LTL due to both an increase in hydrophobicity and pi-pi stacking interactions. Other possible polystyrene-like tails could be implemented and evaluated. One possible drawback of extreme tail modification would be the potential for increased solubility in aqueous solutions. In order to avoid this, the length of the tails must not be decreased in order to add function groups. A fully poly-aromatic tail would have the added benefit of more favorable interactions with the PS-DVB support, but would also have increased interactions with the aqueous phase through charge-induced dipole and dipole-induced dipole interactions.

As stated previously, IMAC is the next logical direction for this work. IMAC would allow investigation of the LTL system through a new affinity-ligand system. IMAC is commonly used to purify proteins that have been engineered with poly-histidine tags. As the C-CP fibers already operate in the turbulent flow regime, the kinetics governing the affinity action would be favorable. Both the LTL and the base fiber material are stable under the aqueous pH range, allowing IMAC elution by a simple change in solvent system pH. More sensitive quantification of available/active surface bound LTL can be accomplished through metal chelation. This is important because to this point protein capture

has been used to evaluated LTL this parameter, and the small metal ions do not have similar steric concerns to the much larger proteins.

REFERENCES

(1) Chang, M. S.; Ji, Q.; Zhang, J.; El-Shourbagy, T. A. *Drug Development Research* **2007**, *68*, 107.

(2) Leader, B.; Baca, Q. J.; Golan, D. E. *Nature Reviews Drug Discovery* **2008**, *7*, 21.

(3) Carter, P. J. *Experimental cell research* **2011**, *317*, 1261.

(4) Gooley, A. A.; Hughes, G.; Humphery-Smith, I.; Williams, K. L.; Hochstrasser, D. F. *Biotechnology* **1996**, *14*, 1.

(5) Young, B. L.; Mlamla, Z.; Gqamana, P. P.; Smit, S.; Roberts, T.; Peter, J.; Theron, G.; Govender, U.; Dheda, K.; Blackburn, J. *European Respiratory Journal* **2014**, *43*, 1719.

(6) Tiberti, N.; Hainard, A.; Lejon, V.; Robin, X.; Ngoyi, D. M.; Turck, N.; Matovu, E.; Enyaru, J.; Ndung'u, J. M.; Scherl, A. *Molecular & Cellular Proteomics* **2010**, *9*, 2783.

(7) Bornhorst, J. A.; Falke, J. J. *Methods in enzymology* **2000**, *326*, 245.

(8) Luo, L.-Y.; Shan, S. J.; Elliott, M. B.; Soosaipillai, A.; Diamandis, E. P. *Clinical Cancer Research* **2006**, *12*, 742.

(9) Papandreou, M.; Persani, L.; Asteria, C.; Ronin, C.; Beck-Peccoz, P. *The Journal of Clinical Endocrinology & Metabolism* **1993**, *77*, 393.

(10) Lee, L. Y.; Hincapie, M.; Packer, N.; Baker, M. S.; Hancock, W. S.; Fanayan, S. *Journal of separation science* **2012**, *35*, 2445.

(11) Qiu, R.; Regnier, F. E. *Analytical chemistry* **2005**, *77*, 2802.

(12) Zatirakha, A.; Smolenkov, A.; Shpigun, O. *Analytica chimica acta* **2016**, *904*, 33.

(13) Schoenmakers, P. J.; van Molle, S.; Hayes, C. M.; Uunk, L. G. *Analytica chimica acta* **1991**, *250*, 1.

(14) Boersema, P. J.; Divecha, N.; Heck, A. J.; Mohammed, S. *Journal of proteome research* **2007**, *6*, 937.

(15) Hong, P.; Koza, S.; Bouvier, E. S. *Journal of liquid chromatography & related technologies* **2012**, *35*, 2923.

(16) Regnier, F. E.; Gooding, K. M. *Analytical biochemistry* **1980**, *103*, 1.

(17) Shi, Q.-H.; Tian, Y.; Dong, X.-Y.; Bai, S.; Sun, Y. *Biochemical engineering journal* **2003**, *16*, 317.

(18) Gómez-Ordóñez, E.; Alonso, E.; Rupérez, P. *Talanta* **2010**, *82*, 1313.

(19) Hradil, J.; Švec, F. *Reactive polymers* **1990**, *13*, 43.

(20) Djordjevic, N.; Laub, R.; Kopecni, M.; Milonjic, S. *Analytical Chemistry* **1986**, *58*, 1395.

(21) Pohl, C.; Saini, C. *Journal of Chromatography A* **2008**, *1213*, 37.

(22) Linde, S.; Welinder, B. *Journal of Chromatography A* **1991**, *548*, 195.

(23) Claessens, H.; Van Straten, M. *Journal of Chromatography A* **2004**, *1060*, 23.

(24) Chuang, S.-C.; Chang, C.-Y.; Liu, C.-Y. *Journal of Chromatography A* **2004**, *1044*, 229.
(25) Barkley, D.; Dahms, T.; Villeneuve, K. *Journal of Chromatography A* **1987**, *395*, 631.
(26) Nelson, D. K.; Marcus, R. K. *Journal of chromatographic science* **2003**, *41*, 475.
(27) Marcus, R. K. *Journal of separation science* **2009**, *32*, 695.
(28) Stanelle, R. D.; Mignanelli, M.; Brown, P.; Marcus, R. K. *ANAL BIOANAL CHEM* **2006**, *384*, 250.
(29) Marcus, R. K.; Davis, W. C.; Knippel, B. C.; LaMotte, L.; Hill, T. A.; Perahia, D.; Jenkins, J. D. *Journal of Chromatography A* **2003**, *986*, 17.
(30) Nelson, D. K.; Marcus, R. K. *Anal. Chem.* **2006**, *78*, 8462.
(31) Stanelle, R. D.; Sander, L. C.; Marcus, R. K. *J CHROMATOGR A* **2005**, *1100*, 68.
(32) De Wilde, D.; Detobel, F.; Billen, J.; Deconinck, J.; Desmet, G. *Journal of separation science* **2009**, *32*, 4077.
(33) Wang, Z.; Marcus, R. K. *J CHROMATOGR A* **2014**, *1351*, 82.
(34) Marcus, R. K. *J SEP SCI* **2008**, *31*, 1923.
(35) Hatti-Kaul, R.; Mattiasson, B. *Isolation and purification of proteins*; Marcel Dekker, Inc.: Basel, Switzerland, 2003.
(36) Nelson, D. M.; Marcus, R. K. *Protein and peptide letters* **2006**, *13*, 95.
(37) Stanelle, R. D.; Straut, C. M.; Marcus, R. K. *Journal of chromatographic science* **2007**, *45*, 415.
(38) Stanelle, R. D.; Marcus, R. K. *ANAL BIOANAL CHEM* **2009**, *393*, 273.
(39) Randunu, K. M.; Dimartino, S.; Marcus, R. K. *Journal of separation science* **2012**, *35*, 3270.
(40) Pittman, J. J.; Klep, V.; Luzinov, I.; Marcus, R. K. *Analytical Methods* **2010**, *2*, 461.
(41) Jiang, L.; Jin, Y.; Marcus, R. K. *Journal of Chromatography A* **2015**, *1410*, 200.
(42) Jiang, L.; Marcus, R. K. *Analytical and bioanalytical chemistry* **2016**, *408*, 1373.
(43) Jiang, L.; Marcus, R. K. *Analytical and bioanalytical chemistry* **2015**, *407*, 939.
(44) Schadock-Hewitt, A. J.; Marcus, R. K. *J SEP SCI* **2014**, *37*, 495.
(45) Trang, H. K.; Schadock-Hewitt, A. J.; Jiang, L.; Marcus, R. K. *Journal of Chromatography B* **2016**, *1015*, 92.
(46) Schadock-Hewitt, A. J.; Bruce, T. F.; Marcus, R. K. *Langmuir* **2015**, *31*, 10418.
(47) Schadock-Hewitt, A. J.; Pittman, J. J.; Christensen, K. A.; Marcus, R. K. *Analyst* **2014**, *139*, 2108.
(48) Schadock-Hewitt, A. J.; Marcus, R. K. *J Sep Sci* **2014**, *37*, 3595.
(49) Jiang, L.; Schadock-Hewitt, A. J.; Zhang, L. X.; Marcus, R. K. *Analyst* **2015**, *140*, 1523.

(50) Neue, U. D. *HPLC Columns: Theory, Technology, and Practice*; Wiley, 1997.
(51) Kirkland, J. *J CHROMATOGR A* **2004**, *1060*, 9.
(52) Rafferty, J. L.; Zhang, L.; Siepmann, J. I.; Schure, M. R. *ANAL CHEM* **2007**, *79*, 6551.
(53) Previderè, C.; Micheletti, P.; Perossa, R.; Grignani, P.; Fattorini, P. *INT J LEGAL MED* **2002**, *116*, 334.
(54) Coolen, E. J.; Arts, I. C.; Swennen, E. L.; Bast, A.; Stuart, M. A. C.; Dagnelie, P. C. *J CHROMATOGR B* **2008**, *864*, 43.
(55) Elgar, D. F.; Norris, C. S.; Ayers, J. S.; Pritchard, M.; Otter, D. E.; Palmano, K. P. *J CHROMATOGR A* **2000**, *878*, 183.
(56) Gilar, M.; Olivova, P.; Daly, A. E.; Gebler, J. C. *J SEP SCI* **2005**, *28*, 1694.
(57) Vailaya, A. *J LIQ CHROMATOGR R T* **2005**, *28*, 965.
(58) Broeckhoven, K.; Desmet, G. *TRAC-TREND ANAL CHEM* **2014**, *63*, 65.
(59) Walter, T. H.; Andrews, R. W. *TRAC-TREND ANAL CHEM* **2014**, *63*, 14.
(60) Fekete, S.; Schappler, J.; Veuthey, J.-L.; Guillarme, D. *TRAC-TREND ANAL CHEM* **2014**, *63*, 2.
(61) Borges, E. M.; Volmer, D. A. *J CHROMATOGR SCI* **2015**, *53*, 1107.
(62) Kirkland, J. *LC GC* **1997**, S46.
(63) Sun, Z.; Deng, Y.; Wei, J.; Gu, D.; Tu, B.; Zhao, D. *CHEM MATER* **2011**, *23*, 2176.
(64) Trojer, L.; Bisjak, C. P.; Wieder, W.; Bonn, G. K. *J CHROMATOGR A* **2009**, *1216*, 6303.
(65) Guiochon, G. *J CHROMATOGR A* **2007**, *1168*, 101.
(66) Nelson, D. M.; Marcus, R. K. *ANAL CHEM* **2006**, *78*, 8462.
(67) Dimartino, S.; Boi, C.; Sarti, G. C. *J CHROMATOGR A* **2011**, *1218*, 1677.
(68) Skoog, D. A.; West, D. M.; Holler, F. J. *Fundamentals of Analytical Chemistry*, 1992.
(69) Liu, Z.; Ou, J.; Lin, H.; Wang, H.; Liu, Z.; Dong, J.; Zou, H. *ANAL CHEM* **2014**, *86*, 12334.
(70) Randunu, K. M.; Marcus, R. K. *ANAL BIOANAL CHEM* **2012**, *404*, 721.
(71) Gusev, I.; Huang, X.; Horváth, C. *J CHROMATOGR A* **1999**, *855*, 273.
(72) Liu, K.; Tolley, H. D.; Lee, M. L. *J CHROMATOGR A* **2012**, *1227*, 96.
(73) Walter, T. H.; Andrews, R. W. *TrAC Trends in Analytical Chemistry* **2014**, *63*, 14.
(74) Fekete, S.; Schappler, J.; Veuthey, J.-L.; Guillarme, D. *TrAC Trends in Analytical Chemistry* **2014**, *63*, 2.
(75) Kirkland, J. J.; Truszkowski, F. A.; Dilks, C. H.; Engel, G. S. *Journal of Chromatography A* **2000**, *890*, 3.
(76) Schuster, S. A.; Wagner, B. M.; Boyes, B. E.; Kirkland, J. J. *J. Chromatogr. A* **2013**, *1315*, 118.
(77) Sun, Z. D., Yonghui.Wei, Jing.Gu, Dong.Tu, Bo. Zhoa, Dongyuan. *Chemistry of Materials* **2011**, 2176.

(78) Borges, E. V., Dietrich. *Journal of Chromatographic Science* **2015**, 1107.
(79) Kirkland, J. J. *LCGC* **1997**, S46.
(80) Cunico, R. L.; Gooding, K. M.; Wehr, T. *Basic HPLC and CE of Biomolecules*; Bay Bioanalytical Laboratory: Richmond, CA, 1998.
(81) Sober, H.; Peterson, E. A. *Journal of the American Chemical Society* **1956**, 751.
(82) Peterson, E. A.; Sober, H. A. Fed. Proc., 1954; Vol. 13, p 273.
(83) Gooding, K. R., Fred. *HPLC of Biological Macro-Molecules, Revised and Expanded*; Marcel Deckker, 2002; Vol. 87.
(84) Yang, Y.-b. H., Kervin.Kindsvater, John. *Journal of Chromatography A* **1996**, *723*, 1.
(85) Chambers, T. K. F., James. *Journal of Chromatography A* **1998**, 139.
(86) Daley, R.; Daley, S. *Organic Chemistry, Part 3*, 2005.
(87) Zhao, G.; Chen, S.; Chen, X.-W.; He, R.-H. *Anal Bioanal Chem* **2013**, *405*, 5353.
(88) Leonard, M. F., C.Coq-Leonard, I.Dellacherie, E. *Langmuir* **1995**, *11*, 2344.
(89) Leonard, M. F., C.Dellacherie, E. *Journal of Chromatography B* **1995**, *664*, 39.
(90) Nash, D. C. C., Howard A. *Journal of Chromatography A* **1997**, *766*, 55.
(91) Nash, D. C.; McCreath, G. E.; Chase, H. A. *Journal of Chromatography A* **1997**, *758*, 53.
(92) Walsh, G. *Nature Biotechnology* **2010**, *28*, 917.
(93) Ladisch, M. R. *Bioseparations Engineering: Principles, Practice, and Economics*; Wiley-Interscience: New York, 2001.
(94) Carta, G.; Jungbauer, A. *Protein Chromatography: Process Development and Scale-Up*; Wiley-VCH: Weinheim, 2010.
(95) Marcus, R. K.; Davis, W. C.; Knippel, B. C.; LaMotte, L.; Hill, T. A.; Perahia, D.; Jenkins, J. D. *J. Chromatogr. A* **2003**, *986*, 17.
(96) Stanelle, R. D.; Mignanelli, M.; Brown, P.; Marcus, R. K. *Anal. Bioanal. Chem.* **2006**, *384*, 250.
(97) Burdette, C. Q.; Marcus, R. K. *Analyst* **2013**, *138*, 1098.
(98) Burdette, C. Q.; Marcus, R. K. *J. Am. Soc. Mass Spectrom.* **2013**, *24*, 975.
(99) Manard, B. T.; Marcus, R. K. *J. Am. Soc. Mass Spectrom.* **2012**, *23*, 1419.
(100) Randunu, K. M.; Marcus, R. K. *Biotechnol. Prog.* **2013**, *29*, 1222.
(101) Wang, Z.; Marcus, R. K. *Biotechnol. Progr.* **2015**, *15*, 97.
(102) Schadock-Hewitt, A. J.; Pittman, J. J.; Christensen, K. A.; Marcus, R. K. *Analyst* **2014**, *139*, 2108.
(103) Jiang, L.; Schadock-Hewitt, A. J.; Zhang, L. X.; Marcus, R. K. *Analyst* **2015**, *140*, 1523.
(104) Schadock-Hewitt, A. J.; Bruce, T.; Marcus, R. K. *Langmuir* **2015**, *31*, 10418.
(105) Wang, Z.; Marcus, R. K. *J. Chromatogr. A* **2014**, *1351*, 82.

(106) Qui, H.; Pan, B.-C.; Zhang, Q.-J.; Zhang, W.-M.; Zhang, Q.-X. *J. Zheijiang Univ. Sci. A* **2009**, *10*, 716.

(107) Gonzalez, M.; Bagatolli, L.; Echabe, I.; Arrondo, J.; Argarana, C.; Cantor, C.; Fidelio, G. *The Journal of Biological Chemistry* **1997**, *272*, 11288.

(108) Acworth, I.; Plante, M.; Bailey, B.; Crafts, C. *Thermo Fisher Scientific, Inc. Publication Number LPN* **2011**, *2931*, 01.